RELIABILITY BASED SEISMIC ASSESSMENT OF UNANCHORED CIRCULAR STEEL STORAGE TANKS

A Thesis Submitted to
the Graduate School of Engineering and Sciences of
İzmir Institute of Technology
In Partial Fulfillment of the Requirements for the Degree of

MASTER OF SCIENCE

in Civil Engineering

by
Nurullah BEKTAŞ

July 2020
İZMİR

ACKNOWLEDGEMENTS

I offer my gratitude to the closest people to me for their help and support during my graduate education without their support I would not reach this level of education!

First of all, I would like to express my gratitude to Assoc. Prof. Dr. Engin AKTAŞ, my supervisor, for his patience, constant guidance, and encouragement during the progress of this thesis.

I would like to thank all my family, especially my mother, Birgül BEKTAŞ, my father, Fazlı BEKTAŞ, and my sister, Neslihan BEKTAŞ, for their endless patience and encouragement in all that I wanted to do about my education.

Finally, but least, I want to express my respect to my friends who helped me during the completion of this study. Thank you all.

ABSTRACT

RELIABILITY BASED SEISMIC ASSESSMENT OF UNANCHORED CIRCULAR STEEL STORAGE TANKS

Since liquid storage tanks are important systems for the safety of industrial facilities, the tightness of these structures and their serviceability are key issues. Therefore, the ability of large liquid storage tanks to withstand damage during earthquakes is of great relevance not only to the engineering profession but also to the safety of society in general. This is because these structures often form an important part of a community's lifeline and therefore should remain in use in emergency situations. In addition, since the content stored in some facilities could be hazardous, in this case, necessary measures must be taken against accidental infiltration. Due to the importance of storage tanks for society, there are many studies and standards in the literature on the behavior of liquid storage tanks. The most detailed method is the incremental dynamic analysis, which considers the time history analysis within a finite element model for the seismic analysis of unanchored circular steel liquid storage tanks to assess performance.

In this study, a performance-based study was conducted on the dynamic behavior of an unanchored circular steel liquid storage tank in order to consider possible improvements in the design phase of the model to withstand earthquakes. It is assumed that the tanks stand on a rigid foundation and are exposed to one-way horizontal ground motion. The main purpose of the study is to determine the performance of the structure for certain failure criteria by using the engineering program ABAQUS to perform reliability-based analyzes of the model.

Keywords: Liquid Storage Tanks, Unanchored, Nonlinear Seismic Response, Hydrodynamic Response, Finite Element Model, Time-History Analysis, Fragility Curves

ÖZET

ANKRAJSIZ DAİRESEL ÇELİK DEPOLAMA TANKLARININ GÜVENİLİRLİK TABANLI SİSMİK DEĞERLENDİRMESİ

Sıvı depolama tankları, endüstriyel tesislerin güvenliği için önemli sistemler olduğundan, bu yapıların sağlamlığı ve hizmet verebilirliği kilit konulardır. Bu nedenle, büyük sıvı depolama tanklarının depremler sırasında hasara dayanma kabiliyeti sadece mühendislik mesleği için değil, aynı zamanda genel olarak toplumun güvenliği için de büyük önem taşımaktadır. Bunun nedeni, bu yapıların genellikle bir toplumun yaşam çizgisinin önemli bir parçasını oluşturması ve bu nedenle acil durumlarda kullanımda kalmalarıdır. Ayrıca, bazı tesislerde depolanan içerik tehlikeli olabileceğinden, bu durumda, kazara sızmaya karşı gerekli önlemler alınmalıdır. Depolama tanklarının toplum için önemi nedeniyle, literatürde sıvı depolama tanklarının davranışı hakkında birçok çalışma ve standart bulunmaktadır. Ankrajsız dairesel çelik sıvı depolama tanklarının performansını değerlendirmek için en ayrıntılı yöntem olan artımlı dinamik analiz methodu zaman geçmişi analizlerinin sonlu elemanlar modeline uygulanmasıyla elde edilir.

Bu çalışmada, depremlere dayanacak modelin tasarım aşamasında olası gelişmeleri dikkate almak için, sabit olmayan bir dairesel çelik sıvı depolama tankının dinamik davranışı üzerinde performansa dayalı bir çalışma yapılmıştır. Tankların rijid bir temel üzerinde durduğu ve tek yönlü yatay yer hareketine maruz kaldığı varsayılmaktadır. Çalışmanın temel amacı, modelin güvenilirlik tabanlı analizlerini yapmak için ABAQUS mühendislik programını kullanarak belirli başarısızlık kriterleri için yapının performansını belirlemektir.

Anahtar Kelimeler: Sıvı Depolama Tankları, Ankrajsız, Doğrusal Olmayan Sismik Tepki, Hidrodinamik Yanıt, Sonlu Elemanlar Modeli, Zaman-Geçmiş Analizi, Kırılganlık Eğrileri

TABLE OF CONTENTS

LIST OF FIGURES

Figure **Page**

Figure **Page**

Figure **Page**

LIST OF TABLES

Table **Page**

LIST OF ABBREVIATIONS

AIJ	Architectural Institute of Japan
ALA	American Lifelines Alliance
ALE	Arbitrary Lagrangian Eulerian
API	American Petroleum Institute
ASCE	American Society of Civil Engineering
AWWA	American Water Works Association
BOCA	Building Officials and Code Administrators
CEL	Coupled Eulerian Lagrangian
CEN	Comité Européen de Normalisation (European Standardisation Organization)
COSMOS	Consortium of Organizations for Strong Motion Observation Systems
DM	Damage Measure
DS	Damage State
EDP	Engineering Demand Parameter
EFB	Elephant's Foot Buckling
ET	Endurance Time
FEA	Finite Element Analysis
FEM	Finite Element Model
FEMA	Federal Emergency Management Agency
FSI	Fluid-Structure Interaction
HAZUS	Hazards United States
IBC	International Building Code
IDA	Incremental Dynamic Analysis
IM	Intensity Measure
LNG	Liquid Natural Gas
NZSEE	New Zealand Society of Earthquake Engineering
PBEE	Performance-Based Earthquake Engineering
PEER	Pacific Earthquake Engineering Research
PGA	Peak Ground Acceleration
PGV	Peak Ground Velocity

SBC	Southern Building Code
SPO	Static Pushover
UBC	Uniform Building Code

CHAPTER 1

INTRODUCTION

Unanchored circular steel storage tanks produced from welded thin plates are generally utilized for liquids like water, oil-based commodities, chemical items, and many different ingredients. These sorts of tanks are appropriate to utilize both industrial and residential locations. Liquid storage tanks are utilized in water supply facilities, nuclear plants, oil and gas industries for storage of oil, liquid natural gas (LNG), etc. Damage of these structures in quakes can prompt to direct or possible indirect consequences, which shows the importance of these structures. In this manner, they should be intended to withstand under seismic excitation safely. Failure of such systems may prompt the loss of essential substances and obstruct firefighting endeavours following destructive earthquakes.

The number of available refineries at all over the world shows the possible consequences of earthquake events. The following Figure 1.1 shows the places of petrochemical plants across the globe. As seen in Figure 1.2, some of the petrochemical facilities shown in Figure 1.1 are at the seismically hazardous locations.

Figure 1.1 Refinery map all over the word

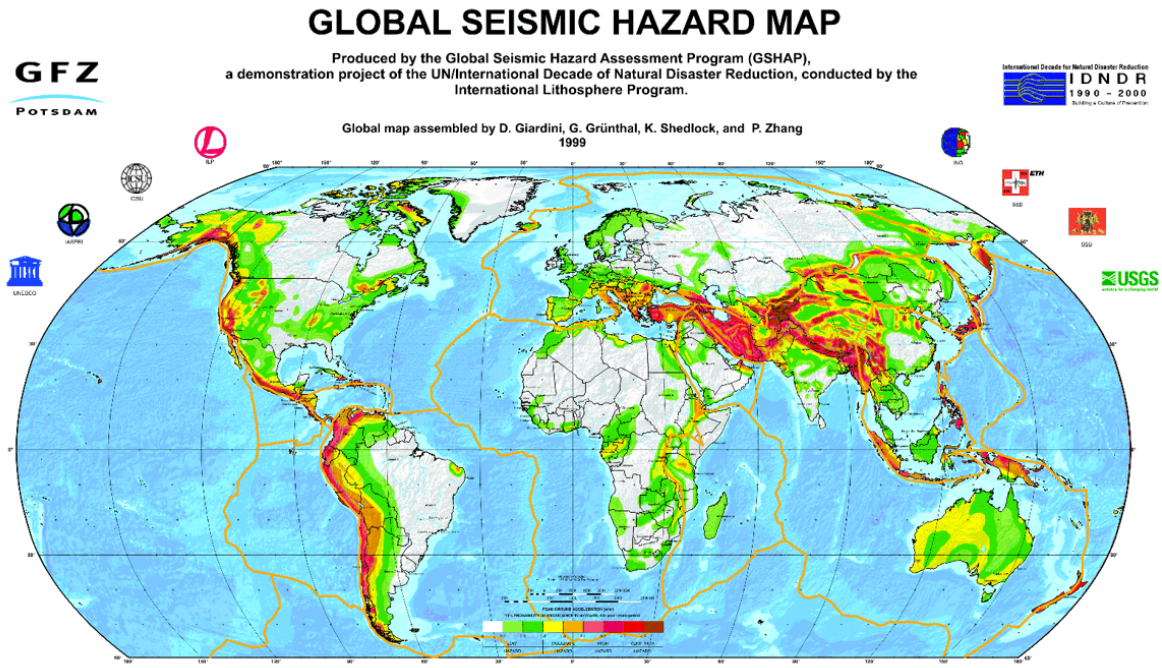

Figure 1.2 Global seismic hazard map

Numerous investigations have been considered to exhibit the behaviour of liquid storage tanks. Some of the main contributions to this research field are Haroun & Housner (1981), Housner (1954) and Malhotra (1992). Elastic and elastoplastic buckling have done significant damage to essential structures during seismic events. Therefore, researchers seek to develop accurate and useful storage tank analysis methods, because modelling liquid and analyzing whole structure with liquid is setting aside much effort to get a structural response. At the early stages of studying this issue, the tank assumed to be rigid and settled on a rigid foundation. Late studies have revealed the significance of the flexibility of the tank wall, tank-foundation interaction, and tank-fluid interaction. When considering fluid-structure interaction, it is required to account for hydrostatic and hydrodynamic pressure. The calculation of the hydrodynamic liquid pressure on the storage tank wall is the utmost issue at the structural analysis phase. Interactions are the most complicated part of analyzing liquid storage tanks.

Basic models and Finite Element Analysis (FEA) solutions were proposed to estimate possible failure criteria of the structure under seismic loading. With the increasing efficiency of computers and the improvement of the FEA empowered to run detailed analyses.

The liquid behaviour for rigid tanks, as well as flexible tanks, explained by the superposition of two components of hydrodynamic actions of the liquid, which have

convective and impulsive components. The impulsive component of hydrodynamic action of liquid, which represents the part of the fluid that is taking consider to move with tank wall as a rigidly connected mass. At the same time, the convective component of hydrodynamic action creates sloshing action within the storage tank.

1.1 Objective and Scope

The main objective of this study is to comprehensively investigate the performance of the unanchored circular steel liquid storage tank supported on a rigid foundation under lateral earthquake excitation. For this purpose, the finite element analysis (FEA) approach is utilized for seismic action. Therefore, ABAQUS software, which is capable of investigating the fluid-structure and the soil structure interaction through nonlinear behavior of geometry and material, has been used to create a more realistic FEA model of an unanchored cylindrical steel liquid storage tank. The liquid-structure interaction is defined by considering the impulsive component of the hydrodynamic action of liquid on the wall and bottom of the tank. As explained by Chen (2010) and Ghaemmaghami (2002), the effect of impulsive hydrodynamic pressure component of the liquid pressure on the flexibility of the storage tank is considered, and convective hydrodynamic pressure component could be ignored because the upper portion of the model highly affected by convective hydrodynamic pressure component.

Moreover, Incremental Dynamic Analysis (IDA) is an effective methodology to get the response of the model, is utilized to evaluate the performance of the structure under all these forces. The results obtained with IDA are processed for a reliability-based performance assessment using fragility curves. The detailed objectives of this study are summarized as follows;

1. Investigation of the impulsive pressure distribution of circular liquid storage tanks on the tank wall and base as the effect of fluid-structure interaction.
2. Investigating the soil-structure interaction of a flexible unanchored circular steel liquid storage tank held on the rigid foundation.
3. Developing a three-dimensional finite element model of in the time domain for nonlinear dynamic analysis of an unanchored circular steel liquid storage tank.

4. Scaling selected ground motion record set for incremental dynamic analysis (IDA).
5. Analyzing the unanchored circular steel liquid storage tank under horizontal accelerogram records to investigate compressive meridional stress at the bottom course of the tank wall and uplift of the base plate of tank.
6. In particular, this study generated fragility curves based on the selected failure criteria with finite element analysis.

1.2 Thesis Layout

Based on the objectives and scope of the research, this study consists of seven chapters.

Chapter 1 provides a brief introduction to the structures containing liquids, the scope, and the purpose of the present thesis.

Chapter 2 provides an extensive literature review of the seismic behavior of liquid storage tanks and discusses the types of liquid storage tanks, the behavior of storage tanks at historical earthquakes, the previous research, and developed model on the seismic response of liquid-containing structures and design codes and standards.

Chapter 3 describes an extensive study about types of failure modes and failure criteria from past earthquakes for circular liquid storage tanks, as discussed in section 2.3.

In Chapter 4, the tank and foundation are modeled by using the finite element method, and an analytical approach is used to evaluate impulsive hydrodynamic liquid pressure at the wall and base of the tank. For the dynamic analysis of the model, the general-purpose finite element analysis software ABAQUS is used. For the analytical calculation of the impulsive hydrodynamic pressure, theoretical explanation, and calculations made. Moreover, the nonlinear properties of the material and finite element formulation of the three-dimensional liquid storage tank are explained.

In Chapter 5, the general purpose of the IDA is explained. The assessment of liquid storage tank explained step by step with considering incremental dynamic analysis philosophy. Then, the selection and scaling of the ground motion data procedure are described. Consequently, the IDA results have shown for selected failure criteria.

Chapter 6 describes an extensive study about the performance-based earthquake engineering concept and development of liquid storage tanks' fragility curves. The damage state definition and fragility curves of the selected failure criteria explained.

In Chapter 7, a summary and the major conclusions drawn in this study are explained. Also, this chapter presents some recommendations for future studies.

CHAPTER 2

LITERATURE REVIEW

2.1 Introduction

This chapter presents a literature review on liquid storage tank seismic response. In addition to the analysis approaches, the observed performance of these sorts of tanks in earthquakes has been described. A comprehensive literature review has been explained the importance of previous studies on the dynamic analysis of liquid storage tanks. Finally, a summary of the design guidelines used for the design of liquid storage tanks has been made. Overall, this chapter aims to provide an overview of liquid storage tank dynamic behavior formed during earthquakes.

2.2 Types of Approaches for Analysis of Liquid Storage Tanks

There are numerous types of tanks for liquid storage in the literature. However, the number of cylindrical ground supported storage tanks is more common than other types of storage tanks since, as explained by Çelik et al. (2019), the design of the cylindrical liquid storage tank is more straightforward, and they are efficient in resisting the hydrostatic pressure. Also, the construction of the circular ground supported liquid storage tanks is more practical than others.

Concerning analysis approaches of ground supported tanks, these can be classified into three different main classes. (I) Rigid & Flexible Storage Tanks, (II) Anchored & Unanchored Storage Tanks, (III) Rigidly & Flexibly Supported Storage Tanks.

(I) Rigid & Flexible Storage Tanks: In order to improve seismic safety and reduce the risk of liquid storage tank damage or failure, theoretical studies supported by experimental studies shown the behavior of liquid storage tanks by Haroun (1983) and Haroun & Housner (1981). In the beginning, liquid storage tanks' shell has been accepted as rigid in the analysis, as shown in Figure 2.1. However, the importance of flexible acceptance in the analysis was demonstrated by comparing the response calculated by flexible acceptance of storage tanks with experimental studies Haroun (1983) and Haroun

& Housner (1981). Besides, many simplified models have taken into account structural flexibility when developing accurate and simpler methods such as Malhotra (1992).

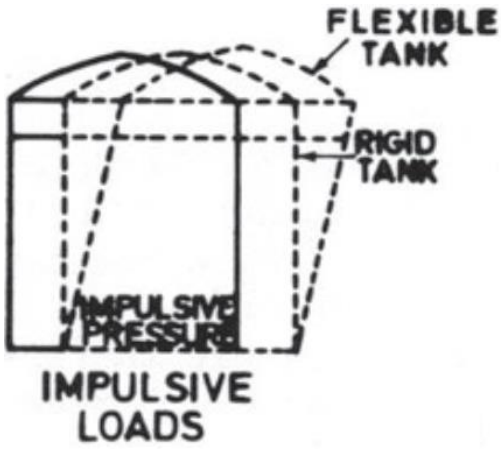

Figure 2.1 Response of a rigid and flexible liquid storage tank under impulsive loads (Barros, 1987)

(II) Anchored & Unanchored Storage Tanks: One of the differences in analysis between anchored and unanchored liquid storage tanks is the evaluation of overturning moments. In the anchored tanks, the overturning moments are evaluated above the base plate; however, in the unanchored tanks, the overturning moment evaluated below the base plate. Also, the hydrodynamic pressure, the uplift, and the subsequent rocking motion could be considered at the base of the unanchored liquid storage tanks. However, the anchored liquid storage tank analysis disregards the soil-structure interaction and is often disregards the base plate of the storage tank, as shown in Figure 2.2. Also, the possible anchored liquid storage tank is shown in Figure 2.3. However, the unanchored liquid storage tanks consider the interaction between foundation and soil to capture a realistic response of the structure, as shown in Figure 2.4.

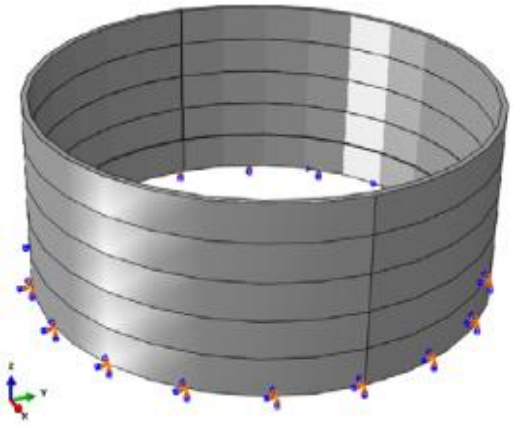

Figure 2.2 An anchored circular liquid storage tank model made in ABAQUS (Tavano, 2011)

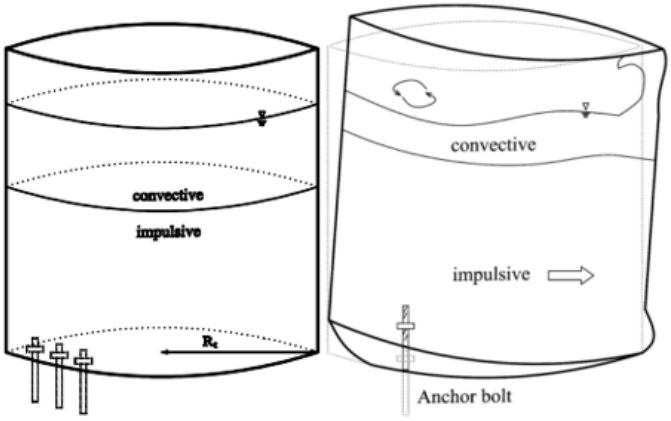

Figure 2.3 Anchored liquid storage tank (Bakalis, 2018)

(III) Rigidly & Flexibly Supported Storage Tanks: The effect of the soil-structure interaction on the flexibly and rigidly supported liquid storage tanks is explained in NZSEE (2009) and CEN (2006). API (2007) also considers the soil-structure interaction effect at liquid storage tanks during the seismic response. “It seems that an overestimation of the foundation stiffness leads to results on the safe side. It has to be kept in mind, though, that for a soft foundation (with low shear wave velocity of the underlying soil), the seismic excitation might be significantly stronger due to local site effects” Koller & Malhotra (2004). Also, Malhotra (1997) performed nonlinear pushover analysis to unanchored liquid storage tanks considering various foundation stiffnesses and observed that assumed foundation stiffness changes the moment-curvature relationship of the storage tank. Besides, a sample response of a cylindrical liquid storage tank on the rigid and flexible foundation during the earthquake is as indicated in Figure 2.4. The results

indicate a distinction between whether the tank is supported by a rigid concrete foundation, a concrete ring, or a compacted soil. Furthermore, “for the same input motion, as the flexibility of the ground increases, the fundamental period of the tank-fluid system and the total damping increase, reducing the peak force response” CEN (2006). In addition, as assumed by Eurocode 8, the convective component of the hydrodynamic action does not affect the soil-structure interaction.

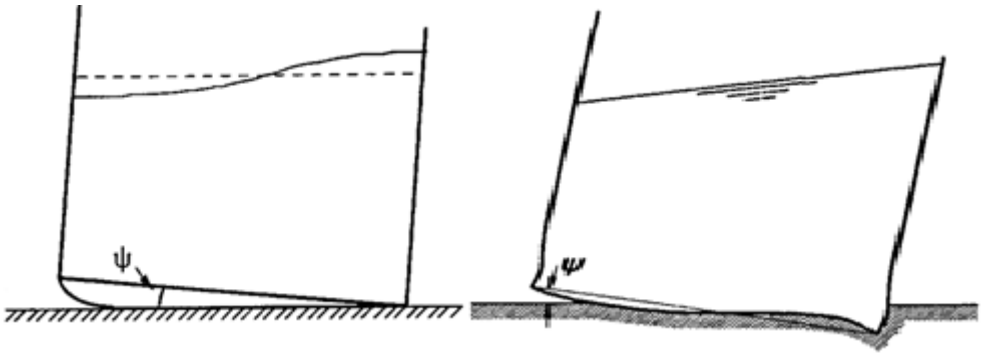

(a) (b)

Figure 2.4 (a) Rigidly supported unanchored liquid storage tank (Malhotra and Veletsos, 1994c), (b) Flexibly supported unanchored liquid storage tank (Malhotra, 1995)

2.3 Damage of Liquid Storage Tanks in Historical Earthquakes

The seismic performance of liquid storage tanks is important beyond the value of liquid stored and storage tanks. Themselves, as shown in Table 2.1, shows many significant earthquakes in various parts of the world. The impact of such earthquakes on liquid storage tanks are described in detail below. These significant earthquakes could be considered to determine failure types and possible consequences of damage at liquid storage tanks under real seismic excitation. Also, the critical overview of the dynamic performance of liquid storage tanks during past earthquakes is the main contribution in defining possible weak points of these kinds of structures.

Table 2.1 Major historical earthquakes caused damage to storage tanks

ID No.	Earthquake			
	Year	Country	Name	Magnitude
1	1906	United States	San Francisco	7.9
2	1933	United States	Long Beach, California	6.4
3	1952	United States	Kern County, California	7.3
4	1960	Chile	Valvida (Great Chilean)	9.5
5	1964	United States	Prince William Sound, Alaska	9.2
6	1964	Japan	Niigata	7.6
7	1971	United States	San Fernando	6.6
8	1971	United States	San Francisco	6.7
9	1972	Nicaragua	Managua	6.3
10	1978	Japan	Miyagi	7.7
11	1979	United States	Imperial Valley	6.4
12	1980	United States	Greenville, California	5.8
13	1983	United States	Coalinga, California	6.3
14	1985	Chile	Algarrobo	8.0
15	1986	United States	Adak	8.0
16	1987	New Zealand	Edgecumbe	6.5
17	1989	United States	Loma Prieta, California	6.9
18	1991	Panama	Limon	7.7
19	1992	United States	Landers, California	7.3
20	1994	United States	Northridge	6.7
21	1995	Japan	Kobe	6.9
22	1999	Turkey	Kocaeli	7.4
23	2001	India	Gujarat	7.7
24	2003	Iran	Bam	6.6
25	2003	Japan	Tokachi-oki	8.3
26	2007	Peru	Central Peru	8.0
27	2010	Chile	Chile	8.8
28	2011	Japan	Tohoku	9.0
29	2014	United States	Napa Valley, California	6.0

The 1906 San Francisco, USA earthquake is one of the significant earthquakes of all time and the effect of this earthquake on storage tanks explained by Avval (2012), Chen (2010), Ghaemmaghami (2002), NZSEE (2009) and Yazıcı (2008). In this earthquake, the importance of water storage tanks and pipelines well realized. Besides, loss of the petrochemical structures caused large scale environmental disasters. The fuel storage tanks were close to each other, so fire leaped to neighboring storage tanks and increased the damage. Because of the water pipeline ruptures, firefighting was deficient, and fires were spread all over the city.

In the 1933 Long Beach, USA earthquake, several failures were observed in the petrochemical oil productions, refineries, transport facilities, and storage tanks. The

reason for the relatively low number of damage is that most of the tanks were not full during the earthquake, and the soil properties were relatively good. Besides, the observed failures occurred in riveted tanks, as explained in detail by ALA (2001) and D'Amico et al. (2018).

In the 1952 Kern County, USA earthquake followed by many strong aftershocks. The initial seismic excitation occurred close to storage tanks and damages explained by D'Amico et al. (2018) and NZSEE (2009). Damage occurred at pipelines and floating roofs of the storage tanks. The smaller diameter tanks had elephant foot buckling, and an almost full tank was collapsed.

The great 1960 Chilean earthquake is the most significant earthquake that has been recorded. Many elevated tanks failed in this earthquake as reported by ALA (2001), Ghaemmaghami (2002) and Housner (1963). The magnitude of this earthquake considered between 9.4-9.6. However, it is generally considered as 9.5 as reported in Chen (2010).

The 1964 Prince William (Great Alaska), USA earthquake near Prince William Sound, caused significant damage to the oil storage tanks given in Chen (2010), Christovasilis (2006) and D'Amico et al. (2018). This earthquake took the attention of earthquake engineering researchers to develop guidelines for liquid storage tank seismic design. The damages at the smaller tanks were more severe than bigger ones. At some of the tanks, elephant foot buckling and damages to connecting pipes, tank shells, and roof failure were observed. Also, a fire has been observed in some of the tank farms. Finally, one of the essential features of this earthquake is that damage to tank farms occurs simultaneously due to the earthquake, fire, and waves.

The main effect of the 1964 Niigata, Japan earthquake on the storage tanks mentioned by Chen (2010), D'Amico et al. (2018), Lee et al. (2019), Moslemi (2011) and Yazdanian & Ghasemi (2017), was seen at the Showa Oil Co. and the Nippon Oil Co. plants as severe damage. The crude oil tanks in Showa Oil Co. burned out just after the earthquake.

The 1971 San Fernando, USA earthquake reported by Avval (2012), Chen (2010) and Hafez (2012) caused buckling in the shell plates at the steel water tank, and because of the overloading, the differential settlement was seen as foundation failure. Moreover, because of the sloshing phenomena of liquid roof damage had been observed. Besides, the rocking of the storage tank observed during this earthquake.

The 1971 San Francisco, USA earthquake caused roof and upper shell buckling damage at a squat tank, as explained by D'Amico et al. (2018). The primary damages detected were base plate rapture, shell buckling, damage to connections and roof seals at floating roof storage tanks.

The 1972 Managua, Nicaragua earthquake had a few damages on storage tanks, which are uplifting of anchor bolts, local buckling in the top portion of the storage tank, and elephant foot buckling, as explained by D'Amico et al. (2018).

The 1978 Miyagi earthquake in Japan caused serious damage to the oil storage tanks, as explained by D'Amico et al. (2018), Moslemi (2011), Soules (2011) and Vakilazadsarabi (2014). At the connection of the annular bottom plate and tank wall shell with fillet weld, failure occurred. After checks of the earthquake show that the bottom plate of the storage tank was affected by corrosion; therefore, the effective thickness of the shell decreased and led to failure. Moreover, because of the sloshing phenomena at the floating roof tanks, the oil flushed out. Also, there were some foundation settlement type failures, and anchor bolts pull out had been observed.

The 1979 Imperial Valley, USA earthquake caused roof shell separation at the storage tanks and oil spillage as reported by Rammerstorfer et al. (1990) and Yazıcı (2008). Besides, elephant foot buckling and severe damage had been observed.

The 1980 Greenville, USA earthquake affected the wine tanks. As explained by D'Amico et al. (2018), the damages show that the failures are related to the aspect ratio (H/D) of storage tanks. The recorded failure types are elephant's foot buckling, diamond shape buckling, and anchorage failure.

The 1983 Coalinga, USA earthquake had shown the uplifting, sloshing phenomena on the storage tanks, which caused floating ceiling damage, anchorage failure, and elephant foot buckling as reported by Altun (2013) and D'Amico et al. (2018). The recorded failures show the effect of the aspect ratio on elephant foot buckling. Such as when the aspect ratio increases, elephant foot buckling observation increases.

The 1985 Algarrobo, Chile earthquake had caused spillage of liquid and buckling at the upper portion of the storage tank as explained by ASCE (2010) and Soules (2011).

The 1986 Adak, USA earthquake had been observed many failures during seismic excitation, as explanation stated by D'Amico et al. (2018). However, no damage was seen in tanks with an aspect ratio greater than 1.

The 1987 Edgecumbe, New Zealand earthquake affected the industrial sites seriously and also, the effect of this earthquake on tanks explained by D'Amico et al.

(2018) and Dogangun et al. (2009). The spillage and collapse had been observed at the large stainless steel milk silos. Besides, milk containment storage tanks were toppled on their sides, and the pipe system's failure was observed.

The 1989 Loma Prieta, USA earthquake had shown the effect of soil and foundation type on storage tank seismic performance and for the different foundation and soil types different performance levels observed. The observed failure types were elephant foot buckling, the column collapse of the roof slab, panel joint rapture, and floating roof failure explained by Chen (2010) and D'Amico et al. (2018).

The 1991 Limon, Panama earthquake severely damaged the petrochemical storage tanks as reported by D'Amico et al. (2018). One of the main failures of this seismic excitation was the explosion of a storage tank. Also, sloshing had been affected the severe damage at roof and the upper portion of the tank. Besides, the hydrodynamic pressure affects the joint rupture of the steel plate and roof connections. Moreover, total collapse, extensive tilting, floating roof, and elephant foot buckling were observed in some of the tanks.

The 1992 Landers, USA earthquake causes a small amount of damage at water storage tanks, and only two of the water storage tanks had a total failure. The failures occurred because of the sloshing effect on the roof and the seals, as explained by ALA (2001), D'Amico et al. (2018) and NZSEE (2009).

The 1994 Northridge, USA earthquake caused a significant number of damages to storage tanks reported by Chen (2010), D'Amico et al. (2018), Hafez (2012) and Vakilazadsarabi (2014). Damages had been observed at the water tanks, such as floor shell yielding at hinges, roof damage because of sloshing, uplifting of storage tank cause damage of smaller bolted tanks, and total collapse of some tanks.

The 1995 Kobe, Japan earthquake caused a severe effect at the storage tank farm, as explained by Avval (2012), Chen (2010), Christovasilis (2006) and D'Amico et al. (2018). There were no important failures in the liquefied areas because of the piles used underneath the foundations. At the foundations without piles, the differential settlement and tilting of storage tank caused connecting pipe failures and shell buckling failures had been observed.

In the 1999 Kocaeli, Turkey earthquake, six cylindrical tanks with floating roof burned after the quake because of the ignition of the naphtha, and the fire spread to the adjacent tanks, as shown in Figure 2.5 and explained by Bakalis (2018), Chen (2010), Christovasilis (2006) and Dogangun et al. (2009). At one of the water storage tanks,

elephant foot buckling failure had been reported. The floating roof tanks had a joint connection failure at the top cause the overflow of liquid from the tank. The elevated circular liquid storage tanks' columns failed, caused tilting and loss of ignition, as shown in Figure 2.6.

Figure 2.5 Fire damage at Tüpraş refinery (Sezen and Whittaker, 2004)

Figure 2.6 Damage to oxygen tanks in the Habaş refinery (Sezen and Whittaker, 2004)

The 2001 Gujarat, India earthquake caused the failure of the elevated concrete storage tanks with flexural cracks propagation near the base, as explained by ALA (2001).

The effect of the 2003 Bam, Iran earthquake on liquid storage tanks has explained by D'Amico et al. (2018). That earthquake caused elephant's foot buckling, connecting pipe failures, and liquid leakage at the roof wall connection due to sloshing phenomena.

The 2003 Tokachi-oki, Japan earthquake, explained by Bakalis (2018), D'Amico et al. (2018) and Vakilazadsarabi (2014), caused severe fire damage, and sloshing damage to the roof was observed. The main characteristic of this seismic excitation was that the ground excitation had a long period and strong ground motion data. Therefore, strong sloshing phenomena occurred at the storage tanks, which caused severe damage at the upper portion of the storage tank.

The 2007 Central Peru earthquake, explained by D'Amico et al. (2018), caused the elephant's foot buckling and split around the cylindrical storage tank bottom course.

The damage to the storage tanks caused by the 2010 Chilean earthquake explained in D'Amico et al. (2018) and Zareian et al. (2020). The water storage tank collapsed because of the uplift mechanism cause buckling at the storage tank wall.

During the 2011 Tohoku, Japan earthquake liquefaction affected the storage tanks' floating and foundations swept away by tsunami waves and given detail by Bakalis (2018), D'Amico et al. (2018) and Vakilazadsarabi (2014). Also, the sink of the floating roofs' inner parts as a result of sloshing phenomena had been observed.

During the 2014 Napa Valley, USA earthquake, roof damaging because of the sloshing, connecting pipe failure, and anchorage failure of the full tanks were reported by D'Amico et al. (2018).

Based on previous earthquake observations, as explained above, it is inferred that liquid storage tanks may be subjected to high hydrodynamic pressure during earthquakes. These pressures effects damages and failures of liquid storage tanks in the previous earthquakes, as explained in Chapter 3. The response due to seismic loads on the liquid storage tanks, therefore, attracts many practitioners and researchers. The studies on understanding and improving seismic response are presented in section 2.4.

2.4 Previous Research

Dynamic behaviour calculations of liquid storage tanks have begun in the late 1940s. However, the first research was based on the dynamic behaviour of aerospace industry fuel tanks. The key difference between aerospace and civil engineering storage tanks is the model's natural frequency. The natural frequency of the civil engineering storage tanks is less than aerospace engineering storage tanks because the civil engineering tanks are much larger tank aerospace engineering tanks.

Previous researches and studies on either the dynamic response of liquid storage tanks are discussed in this chapter. The literature review is focused on dynamic response analysis and developed structural models. This section summarizes the research importance, key contributions, and conclusions for individual studies.

Early research on storage tanks dates back to the 1950s and focuses on the hydrodynamic effect of fluids on the rigid storage tanks. Housner (1963) developed a model that is the most commonly used one for the modeling and analysis of the liquid storage tanks, as shown in Figure 2.7 and Figure 2.8. Hydrodynamic pressure induced by liquid distinguished by two parts, which are convective and impulsive pressure. The impulsive pressure component of the hydrodynamic pressure moves with the storage tank wall as a rigid connection. However, the convective pressure component creates sloshing of liquid inside of the tank. On this basis, the simplification of hydrodynamic impulsive and convective pressure is made as added masses, as illustrated in Figure 2.8. The impulsive mass connected to the wall rigidly and convective mass connection made by springs. After the 1964 Alaska earthquake, it better understood the storage tank's actual behaviour and the flexibility of the storage tanks considered under seismic excitations.

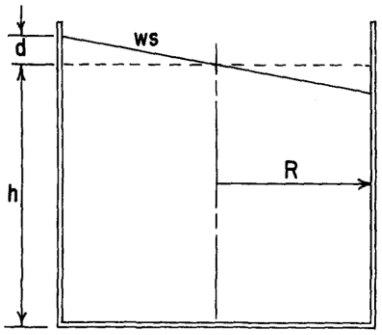

Figure 2.7 Housner's equivalent dynamic model: fluid oscillating in tank (Housner, 1963)

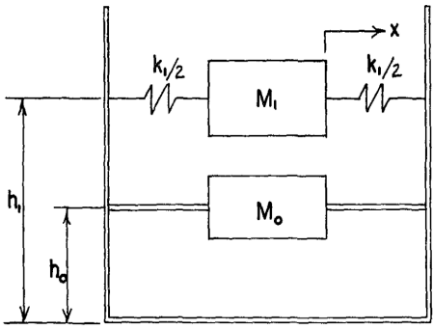

Figure 2.8 Housner's equivalent dynamic model: dynamic model for rigid wall tank (Housner, 1963)

Haroun & Housner (1981) divide the deformable storage tank wall cylindrical finite element meshes, and the water is considered continuous by a boundary solution method. When the wall considered flexible, the evaluated dynamic response is significantly higher than the rigid walls.

Haroun (1983) carried out analytical and experimental research explaining the dynamic response of ground-supported flexible liquid storage tanks. The FEM has used for the liquid-shell system. Liquid region treated as a continuum by the boundary solution and the finite element method applied to the elastic wall. A simplified beam-type soil-structure interaction analysis was utilized to investigate the importance of interaction. The analysis demonstrated by the experimental studies and test results were compared with the rigid storage tank assumption to identify wall flexibility influence. This study provides a more accurate analysis methodology for understanding and improving the dynamic response of liquid storage tanks.

The simplified analyses of unanchored circular steel storage tanks are made by Malhotra (1992). The base plate uplifting response of storage tanks on soil and the rigid foundation was examined by Malhotra (1997), Malhotra & Veletsos (1994a) and Malhotra & Veletsos (1994b). Moreover, the later studies demonstrate the importance of the base uplifting might cause excessive compressive meridional stress on the wall of the storage tank. Also, Malhotra & Veletsos (1994c) studied the 2D model of the cylindrical liquid storage tank as a lumped mass to calculate a structural response, as shown in Figure 2.9 and Figure 2.10.

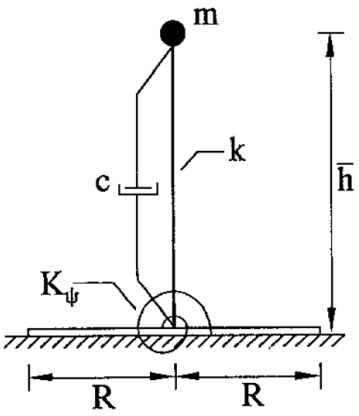

Figure 2.9 Model of unanchored liquid storage tank at rest (Malhotra and Veletsos, 1994c)

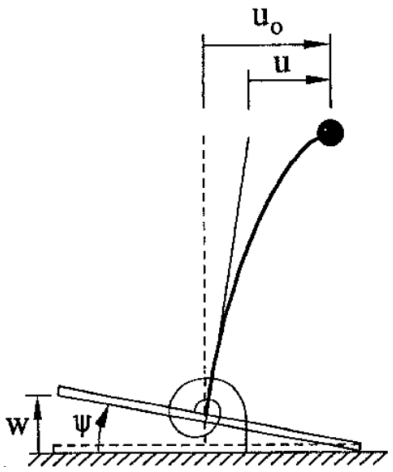

Figure 2.10 Model of unanchored liquid storage tank at seismic analysis (Malhotra and Veletsos, 1994c)

Vathi & Karamanos (2015) suggested a simplified model, which contain rotational spring at the base to consider material and structural nonlinearity of uplift effect, for determination of seismic-induced responses of unanchored steel circular storage tanks. Moreover, the rotational spring properties are valuated from the moment rotation curve of the base of the storage tank using static pushover analysis; for the sake of simplicity of the analysis, the rotational spring properties calculated by considering bilinear stiffness. Finally, for the accuracy of the analysis, the hydrodynamic pressure included at the base and impulsive pressure at the wall considered as a lumped mass.

Cortes et al. (2012) formed a tank model consist of a rigid beam and equivalent rotational spring at OpenSEES. Also, the OpenSEES model time-history analysis' output has compared with ABAQUS output. Phan et al. (2019a) studied unanchored steel storage tank's uplift and elephant foot buckling. ABAQUS had been used to make a pushover analysis of the storage tank to calculate the moment-curvature graph of the system. From the moment-curvature graph, the stiffness of the rotational spring evaluated to determine analysis as a lumped mass 2D model by OpenSEES, as shown in Figure 2.11.

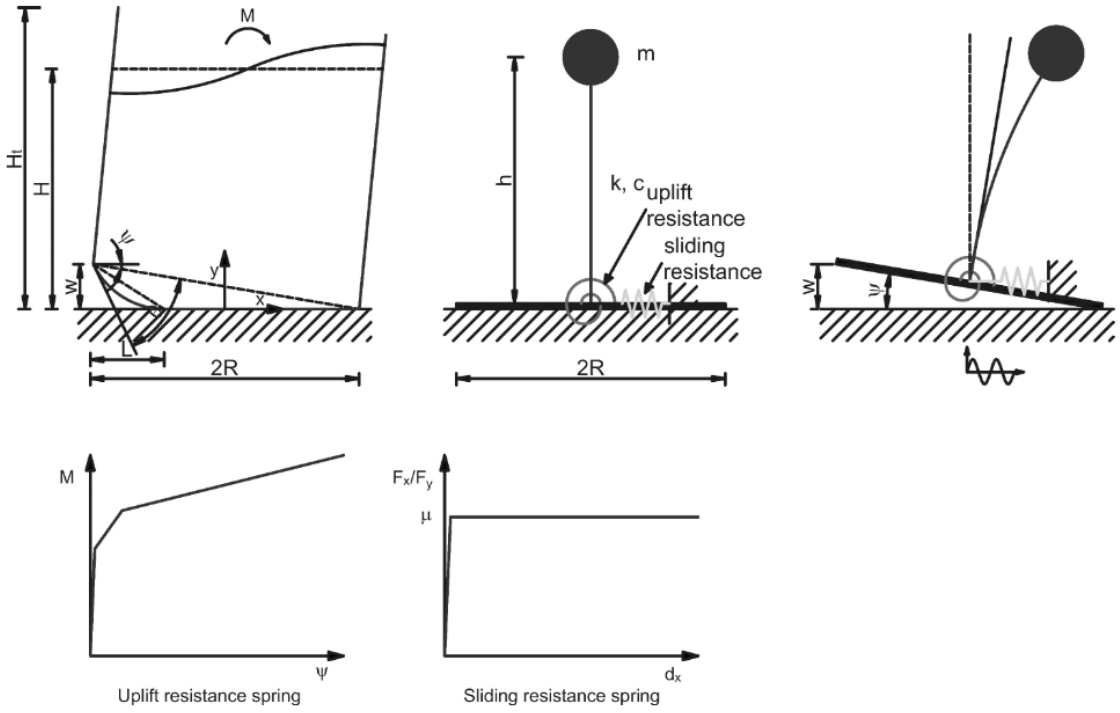

Figure 2.11 Simplified model of the storage tank (Phan et al., 2019a)

Buratti & Tavano (2014), Tavano (2011) and Virella et al. (2005, 2006) modeled hydrodynamic pressure of the storage tank as an added mass model. In this model, masses at each level calculated concerning mesh size, tank height, and impulsive pressure. Because of the impulsive pressure, which is normal to the tank wall, as illustrated in the circumferential pressure representation in Figure 2.12, the added mass connected to the wall and adds inertia in the normal direction, as shown in Figure 2.13. For the creation of the analysis system, Tavano (2011) wrote a MATLAB code to calculate added mass at each mesh and generate ABAQUS input files.

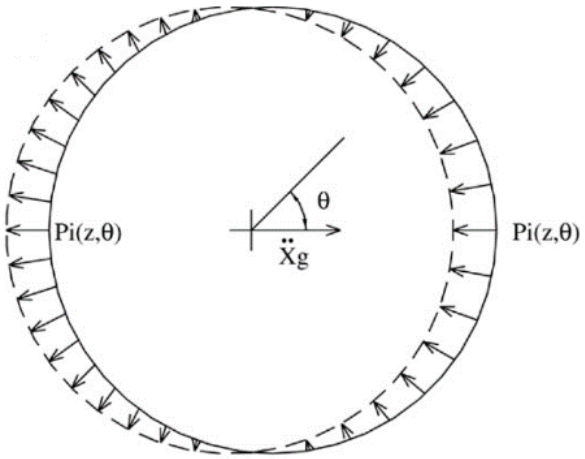

Figure 2.12 Circumferential impulsive pressure distribution (Virella et al., 2006)

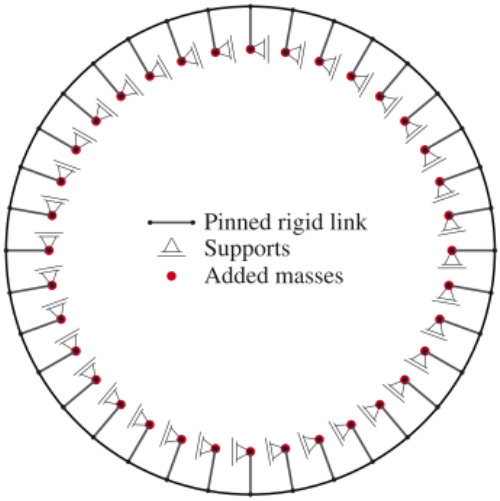

Figure 2.13 Schematic presentation of added mass (Buratti and Tavano, 2014)

Phan & Paolacci (2018), Phan et al. (2019b), Rawat et al. (2015a, 2015b), Rawat et al. (2019a), Rawat et al. (2019b) and Sobhan et al. (2017) have modeled liquid storage tanks with ABAQUS software that capable of finite element analysis. In the analysis, fluid is modeled as acoustic material, as shown in Figure 2.14. The importance of this analysis is the evaluation of sloshing behavior. The interaction between acoustic and wall is defined as tie constraint (surface to surface tie constraint), while the boundary condition for free surface is defined at the liquid's free surface.

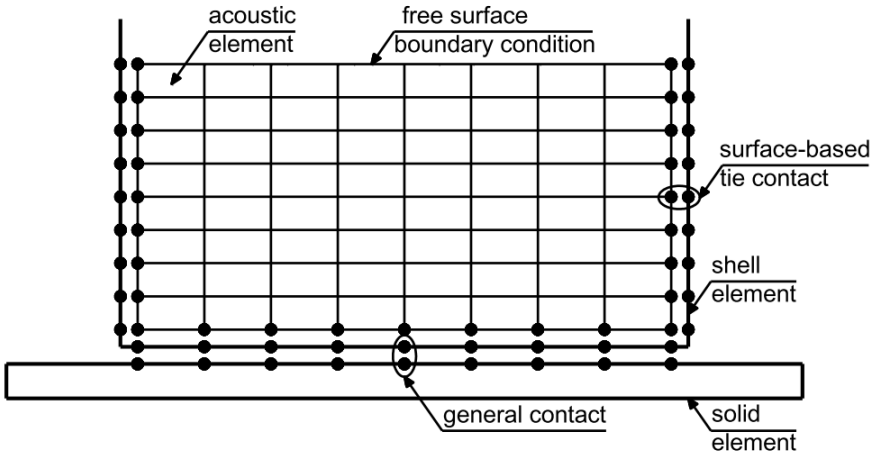

Figure 2.14 Boundary conditions of the coupled acoustic-structure unanchored circular steel liquid storage tank model (Phan et al., 2019b)

Erkmen (2017), Phan & Paolacci (2018), Rawat et al. (2019b) and Vakilazadsarabi (2014) modeled liquid storage tanks using ABAQUS software. Also, Coupled Eulerian-Lagrangian (CEL) and Arbitrary Lagrangian-Eulerian (ALE)

approaches are used for modelling fluid-structure interaction. In the CEL approach, fluid moves inside of the eulerian mesh, and when the liquid amount inside the eulerian mesh is less than 50% of the mesh volume, the fluid-structure interaction is lost, as shown in Figure 2.15. However, in the ALE method, eulerian mesh deform during analysis. Vakilazadsarabi (2014) modeled liquid and air as a eulerian element to sustain fluid-structure interaction (FSI).

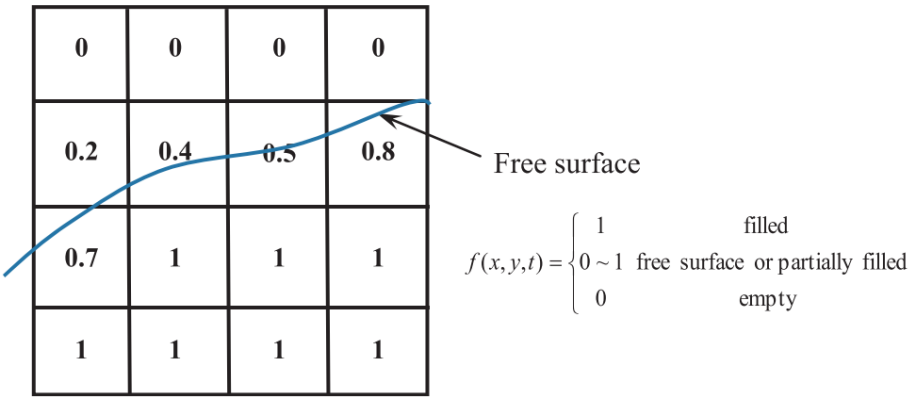

Figure 2.15 The fraction of fluid (f) in each Eulerian element (Rawat et al., 2019b)

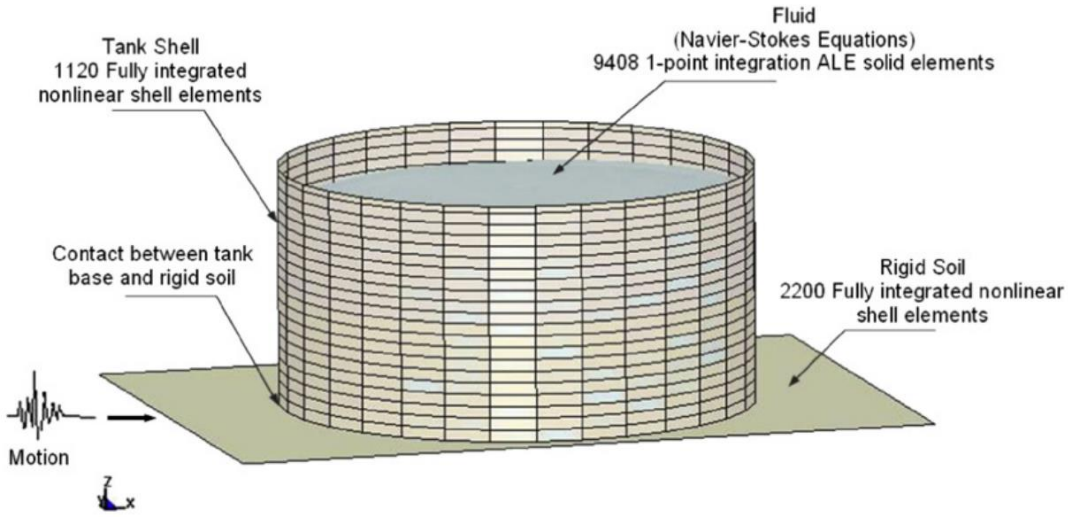

Figure 2.16 ALE method finite element model of unanchored liquid storage tank (Ozdemir et al., 2010)

Several other researchers who provide valuable information in terms of calculating the seismic response of tanks are Ahari et al. (2009), Colombo & Almazán (2019), Jing et al. (2019), Lee et al. (2019), Manos (1982), Ozdemir et al. (2020), Prasad (1989), Priestley (1985), Rashed et al. (2019), Vamvatsikos (2002), Vathi (2017) and Zareian et al. (2020).

2.5 Design Codes and Standards

Several codes and guidelines are currently offered for design and analysis of liquid storage tanks because the petrochemical facilities are generally at the seismic regions. So, there is numerous research on the seismic response analysis of storage tanks. Therefore, many design standards are prepared concerning these studies' outcomes. Most of the standards used to design storage tanks are based on Housner's studies in the 1950s, which are about seismic response analysis of rigid cylindrical storage tanks. The Housner' model contains fluid as an added impulsive and convective mass component. The convective component of the fluid creates sloshing phenomena at the upper edge of the liquid; however, the impulsive component of the fluid moves with storage thanks as a rigid mass.

The American Water Works Association (AWWA) has codes for the design of liquid storage tanks made of both steel and concrete and is one of the principal institutions in the USA for the storage of liquid tanks. For the design of the steel storage tanks, AWWA D100 *Welded Steel Tanks for Water Storage* provided. Moreover, for concrete liquid storage tanks, AWWA D110 and AWWA D115 are provided.

The leading standards for the design of the liquid storage tanks are provided by the American Petroleum Institute (API), which are API 650 *Welded Steel Tanks for Oil Storage* and API 620 *Design and Construction of Large, Welded, Low-pressure Storage Tanks*. The major contribution to this code is based on Housner's study. Also, API 650 and API 620 follow the ASCE 7 *Minimum Design Loads and Associated Criteria for Buildings and Other Structures* loading conditions.

Another most important standard for liquid storage tanks is The New Zealand Code NZSEE (2009) *Seismic Design of Storage Tanks*, which contains rigid and flexible wall storage tank analysis based on the study of Veletsos (1984).

Moreover, Eurocode 8: *Design of structures for earthquake resistance - Part 4: Silos, tanks and pipelines* is based on Veletsos and Yang (1977), which focuses on rigid circular storage tanks. Also, the flexible circular storage tanks analysis part of Eurocode 8 is based on Haroun & Housner (1981), Veletsos (1984) and Veletsos & Ventura (1984). In addition to these studies, a significant contribution to code is made by Malhotra (2000). The impulsive and convective pressure parts of fluid have a detailed explanation in Eurocode 8.

Furthermore, specifications and regulations for the design and detailing of the seismic-induced forces on the liquid storage tanks are laid down in ASCE 7-05 and other codes such as the IBC 2000, UBC 1997, UBC 1994, BOCA 1996 and SBC 1997.

Finally, with respect to given information at the above-given standards, detailed analytical calculations of impulsive hydrodynamic pressure, according to Eurocode 8, are given in section 3 of Chapter 4 in this study. Also, soil-structure interaction properties of the model considered with respect to API 650 is provided with details in section 4 of Chapter 4.

CHAPTER 3

FAILURE MODES AND CRITERIA

Post-earthquake has been revealed many failure criteria on cylindrical liquid storage tanks. Therefore, many engineering design codes and standards contain information about defining the failure criteria of storage tanks and designing to cope with them. Also, steel storage tanks may face many failure modes and suffer extensive damage under seismic and static loading. Major failure modes of steel storage tanks are elephant's foot buckling, diamond shape buckling, secondary buckling, base plate to a wall connection failure, sloshing failure, anchorage failure, tank support system failure, foundation failure, hydrodynamic pressure failure, connecting piping failure, manhole failure, base sliding, overturning failure, etc. These failure criteria were derived from the earthquake excitation on the storage tanks.

3.1 Elephant's Foot Buckling

The elephant's foot buckling, also known as elastic-plastic buckling, is one of the most common failure modes of the circular steel storage tanks. Many researchers, D'Amico et al. (2018) and Phan et al. (2018), Meskouris et al. (2019), Tavano (2011) and Bakalis et al. (2017), stated that the elephant's foot buckling is caused by the high concentration of compressive meridional stress that occurs in the shell when the tank base is uplifted from the ground support. During seismic excitation, the contribution of hydrostatic and hydrodynamic pressure at the storage tank wall prompt higher inner pressure. Local yielding at the storage tank wall can consist of elastic-plastic buckling, which is an elephant's foot buckling, as clearly shown in Figure 3.1. Moreover, the elephant's foot buckling stretches out around the tank perimeter near the lower course because of critical combinations of vertical compressive stress, hoop tensile stress, and high shear stress during seismic loading.

In tanks with variable wall thickness, verification for this mode of buckling should not be limited to the section near the base of the tank, but should extend to the bottom section of all parts of the wall which have a constant thickness (CEN, 2006). Also, if buckling occurs at the mid and high distance along with the height of the tank, is called

the elephant's knee-buckling, as shown in Figure 3.4. However, as explained by Bakalis et al. (2017), the stress limit has not defined for the elephant's knee buckling, and this failure state generally ignored at calculations. In this manner, the lowest course is recognized as the most critical piece of the storage tank for a uniform thickness as well as a variety of steel storage tank thickness.

The formation of the elephant's foot buckling is the result of high circumferential tensile stress due to internal compressive meridional stress and the overturning phenomena caused by the moment of lateral earthquake excitation. Elephant's foot buckling occurs when the compressive meridian stress (σ_m) demand in the tank wall exceeds the critic level. Also, because of the high stress over this critical segment, annular strips cannot convey any further vertical meridional compressive stress.

$$\sigma_m = \sigma_{c1}\left[1-\left(\frac{pR}{sf_y}\right)^2\right]\left(1-\frac{1}{1.12+r^{1.15}}\right)\left[\frac{r+\frac{f_y}{250}}{r+1}\right] \quad (3\text{-}1)$$

$$\sigma_{c1} = 0.6E\frac{s}{R} \quad (3\text{-}2)$$

$$r = \frac{\frac{R}{s}}{400} \quad (3\text{-}3)$$

R: is the radius of the storage tank.

σ_m: maximum vertical membrane stress.

σ_{c1}: The critical buckling stress for cylinders loaded in axial compression.

E: The steel elastic Young modules.

f_y: The yield strength of the tank wall material in MPa.

s: The thickness of the wall course.

p: is the maximum interior pressure, which is the direct sum of the hydrostatic (p_h) and impulsive (p_i) component, on the tank wall in the seismic design situation in MPa.

The above expression is based on nonlinear elastoplastic properties of isotropic material under axisymmetric loading. The ($\frac{pR}{sf_y}$) shows the buckling limit of the shell with

the material yield stress and internal pressure in the circumferential direction. The storage tank wall reaches a buckling limit when the internal pressure is so high that it creates the yielding of the shell in the circumferential direction. In the case of $\frac{pR}{sf_y} = 1$, the storage tank wall vanishes at all.

Figure 3.1 EFB of storage tank during Northridge earthquake in California (Malhotra et al., 2000)

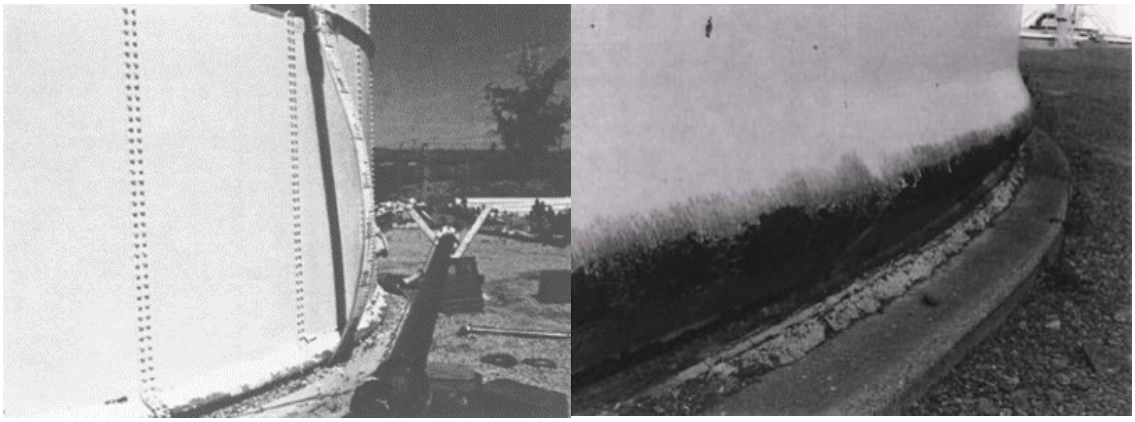

Figure 3.2 EFB at 1982 Landers 1989 Loma Prieta earthquake (NZSEE, 2009)

Figure 3.3 EFB at 1995 Hanshin-Awaji earthquake (AIJ, 2010)

Figure 3.4 Elephant knee buckling (Bakalis, 2018)

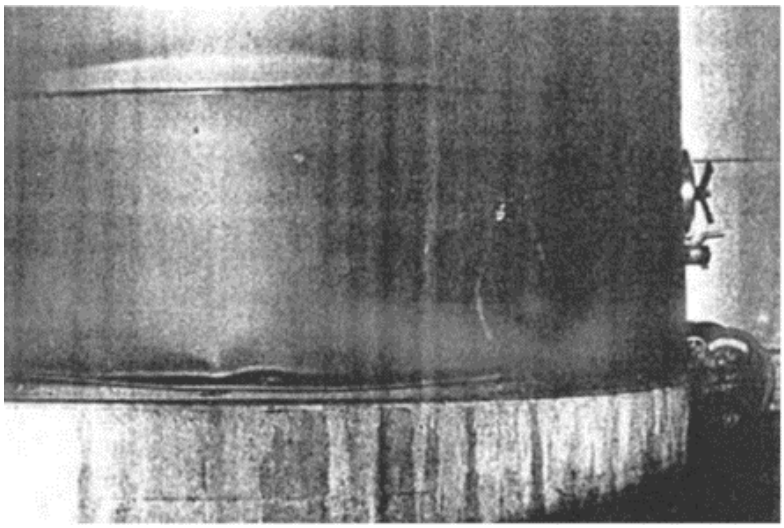

Figure 3.5 Buckled storage tank at EFB mode (Teng and Rotter, 2004)

3.2 Diamond Shape Buckling

The diamond shape buckling is caused by axial compressive stress and roof weight in the generic meridional line of the storage tank wall. These types of failure criteria take place at the low hoop stress and are sensitive to effective imperfection magnitude and internal pressure. The internal pressure decreases the imperfection magnitude and thus tends to rise the buckling stress as explained by Buratti & Tavano (2014). Circumferential variation of the axial stress reduces the probability of coincidence of the maximum stress and the maximum imperfection, again increasing of the buckling stress (Haroun and Al-Kashif, 2005). However, to reach the elastic buckling failure, it is needed to have high compressive meridional stress and low hoop stress induced by hydrostatic and hydrodynamic pressure. Therefore, in addition to the rareness of this situation, the most extensive diamond shape buckling mode is an elastic-plastic failure. The distinctive physical appearance of the diamond shape buckling is no outward protrusion; however, a local wrinkle may occur along with the height of the tank wall, as shown in Figure 3.6, Figure 3.7, and Figure 3.8.

Because of these reasons, the buckling limit as for elastic buckling can be computed by applying an appropriate knockdown factor, $\bar{a}$, to the critical axial compressive stress for an axially loaded, linear-elastic cylinder. The knockdown factor considers defects sensitivity of the bent cylindrical shell and, appropriate values were

given by Haroun (2005) and API (1998), which are 0.2 and 0.33, respectively, as explained by Tavano (2011).

$$f = \bar{a}\,\sigma_{c1} = \bar{a}0.605E\frac{s}{R} \tag{3-4}$$

$$\sigma_{c1} = \frac{E}{\sqrt{3(1-v^2)}}\frac{s}{R} = 0.605E\frac{s}{R} \tag{3-5}$$

Where σ_{c1} is the critical buckling stress for cylinders loaded in axial compression, E is the steel modulus of elasticity, v is the poison's ratio, and s is the wall thickness.

Figure 3.6 Diamond shape buckling occurred during 1980 Livermore (California) earthquake (Rostami and van Gelder, 2017)

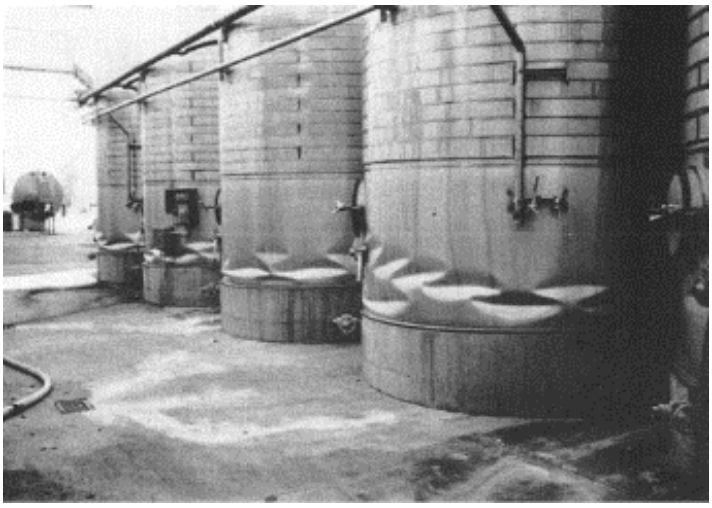

Figure 3.7 Diamond shape buckling of stainless steel wine tanks (NZSEE, 2009)

Figure 3.8 Diamond shape buckling at Hanshin-Awaji Earthquake (AIJ, 2010)

3.3 Secondary Buckling

Another type of buckling for liquid storage tanks is the secondary buckling, which differs from both the diamond shape buckling and the elephant's foot buckling. As mentioned by Rammerstorfer et al. (1990), this third kind of buckling occurs in the top portion of the storage tank, as shown in Figure 3.9. Secondary buckling is the effect of axial compressive forces of the roof and tank wall's. Also, this axial compressive force increases during seismic excitation and create secondary buckling.

Furthermore, Virella et al. (2006) made the initial computational study on the secondary buckling. Also, with respect to Buratti & Tavano (2014), secondary buckling caused by the hydrostatic and hydrodynamic pressure acts in the inward direction at the upper course of the storage tank wall. Besides, Rostami & van Gelder (2017) define the reason for the secondary buckling as a sloshing of liquid motion.

Figure 3.9 Secondary buckling of the shells occurred after the 1999 Izmit earthquake (Rostami and van Gelder, 2017)

3.4 Sloshing Damage

The stimulation of the convective mass for a long period can cause sloshing of the convective component of the liquid, which can damage the upper section and roof of the tank, as shown in Figure 3.10 and Figure 3.11. Several pieces of evidence have been recorded in the literature where the damage to the wall and roof of the liquid storage tanks occurred as a result of liquid sloshing within the tank. The 1971 California and 1999 Kocaeli earthquake-induced waves on the liquid free surface within the storage tank and caused damage to the upper portion of the liquid storage tanks.

Moreover, the ground motion during an earthquake induces waves on the liquid free surface within the liquid storage tanks. When wave height exceeds the available freeboard, sloshing failure occurs. Eurocode 8-4 and API 650 provided empirical formulas to evaluate sloshing wave height, as shown in Equation (3-6) and (3-7), respectively.

$$d_{API-650} = R\, A_f \tag{3-6}$$

Where R is the radius of storage tank and A_f is the acceleration coefficient for sloshing wave height calculation.

$$d_{EC8} = R\, \frac{0.84\, S_a\,(T_{c1}, 0.5\%)}{g} \tag{3-7}$$

Where R is the radius of storage tank, T_{c1} is the first convective period, $S_a\,(T_{c1}, 0.5\%)$ is the first convective mode elastic response spectral acceleration for a defined damping value equal to 0.5% for water and g is the gravitational acceleration.

Figure 3.10 Sloshing damage at 1971 California earthquake (Malhotra et al., 2000)

Figure 3.11 Sloshing damage at 1999 Kocaeli earthquake (Sezen and Whittaker, 2004)

3.5 Base Plate and Wall-to-Base Connection Rupture

During the previous earthquakes, common failure modes of cylindrical steel liquid storage tanks are the elephant's foot buckling at the lower shell course and base plate to wall connection plastic rotation failure. Also, the uplift of the tank may exhibit the base plate to wall welded connection plastic rotation and fracture, as shown in Figure 3.12. These failure types could cause loss of contents because of the connecting pipe or weld fracture. The Eurocode defines maximum plastic rotation limit state at the connection for different damage states.

$$\theta_{pl} = \frac{2w}{L} - \frac{w}{2R} \tag{3-8}$$

Where w is the uplift amount, L is the uplifted length and R is the radius of the tank.

Figure 3.12 Separation of Tank Shell/Floor Weld, 1971 San Fernando earthquake (NZSEE, 2009)

3.6 Base Sliding

The base sliding is not a direct failure type. However, it causes a connection failure of pipes. In base sliding, the total force transferred between the tank and the foundation taking consider to evaluate sliding. Friction between tank and foundation resist sliding. When the calculated seismic base shear, V, exceeds the seismic base shear resistance due to friction, V_s, base sliding occurs. The API (2007) shows seismic base shear resistance of the storage tank as:

$$V_s = \mu \left(W_s + W_r + W_f + W_p\right) * (1.0 - 0.4 * A_v) \tag{3-9}$$

Where W_s is the total weight of the tank shell and appurtenances in Newton, W_r is the weight of fixed tank roof including framing, knuckles, any permanent attachments and 10% of the roof design snow load in Newton, W_f is the weight of the tank bottom in Newton, W_p is the total weight of the tank contents based on the design specific gravity of the product in Newton, A_v is the vertical earthquake acceleration coefficient in %g and μ is the friction coefficient for tank sliding.

3.7 Foundation Failure

One of the major damage types of storage tanks is foundation failure as explained by ALA (2001), which occurs due to the poor foundation conditions. Furthermore, the effects of the foundation's failure are rotation, gross settlement, as shown in Figure 3.13, and excessive sliding. Besides, the failure of the foundation causes excessive local stress concentrations at the base plate of the storage tank, failure of anchorage, failure to connected the pipe, etc.

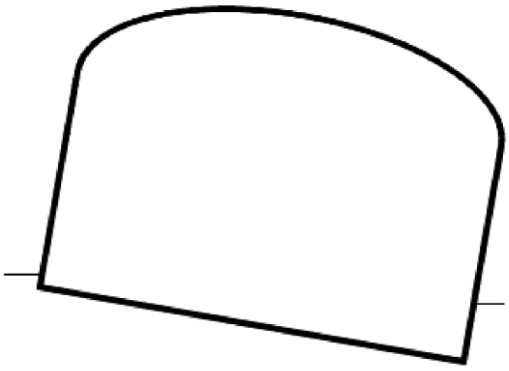

Figure 3.13 Settlements of foundations (Rostami and van Gelder, 2017)

3.8 Hydrodynamic Pressure Failure

Ground motion data excitation to storage tanks increases the tensile hoop stress on the tank, which could cause splitting and leakage. As explained in ALA (2001), this type of failure occurs in riveted type storage tanks and leakage failure seen in riveted joints. The occurrence of this kind of failure arises mostly in the upper course. The American Lifeline Alliance ALA (2001) explains that this failure phenomenon does not

occur directly; however, it affects by extensive hoop stresses at the bottom part of the storage tank, such as an elephant's foot buckling. For example, this failure criterion was seen in the 1989 Loma Prieta and the 1985 Chilean earthquake at concrete tanks.

3.9 Connecting Pipe Failure

Another common failure criteria of storage tanks is connecting piping failure, which occurs mostly at steel storage tanks during seismic ground excitation, as shown in Figure 3.14. The connecting pipe failure occurred many times, especially at the pipe enters from underground to the tank, due to the relative pipe movement with respect to the tank, as explained in ALA (2001). The cause of this failure is generally excessive uplift, buckling, foundation failure, or base sliding of the tank. Moreover, damage to connecting pipes is directly related to the flexibility of connecting pipes.

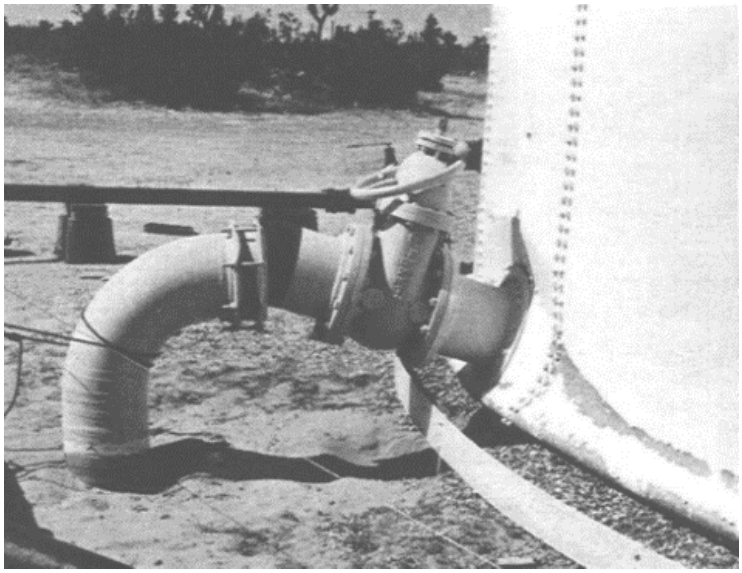

Figure 3.14 Rigid pipe connection, 1992 Landers earthquake (NZSEE, 2009)

3.10 Manhole Failure

When the manhole covers overloaded, manhole failure occurs. Generally, this failure criterion occurs at stainless steel thin-walled wine storage tanks, as explained by ALA (2001). The location of the manholes shown in Figure 3.15 is the same as EFB, as

seen in Figure 3.1. Therefore, this failure criterion occurs at the tank lower course because of the excessive stress increase.

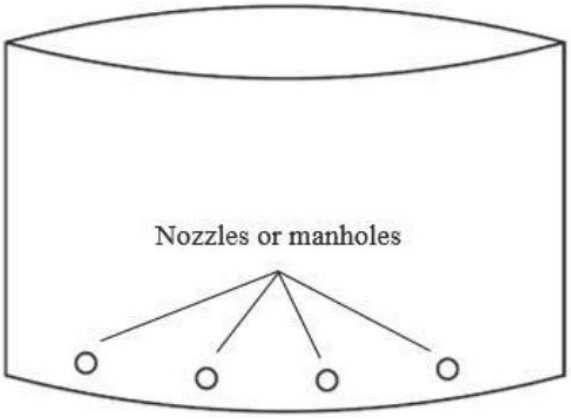

Figure 3.15 The nozzles or manholes of circular liquid storage tank (Bakalis et al., 2015b)

CHAPTER 4

MODELING OF LIQUID STORAGE TANKS

4.1 Introduction

The efficient seismic performance assessment of the liquid storage tanks is based on appropriate structural modeling. Therefore, the finite element method (FEM) is the most reasonable solution technique for creating an accurate model and assessing the performance. Therefore, a three-dimensional finite element analysis model of a cylindrical liquid storage tank is developed for the seismic performance assessment by using ABAQUS software.

In this chapter, the geometrical dimensions of the model and nonlinear material properties are explained. Besides, the definition of the fluid-structure interaction by using impulsive pressure and soil-structure interaction properties are discussed. Also, variety of modeling properties and features of ABAQUS are described. Finally, the modeling procedure for the liquid storage tank explained in detail.

4.2 Model Properties

FEM has been created on a circular rigid foundation to investigate the nonlinear dynamic behavior of the unanchored circular steel liquid storage tank. The geometrical parameters of the tank under examination are outlined in Table 4.1. The storage tank has a cylindrical cross-section of radius R and height H. The tank is filled with liquid up to height H_L and supported on a circular rigid foundation. The thickness of the tank wall varies along with the height, and the tank has a constant base plate thickness. The investigation from the historical earthquakes shows that tanks entirely filled with liquids are more susceptible to damage as explained by Sobhan et al. (2017). Therefore, the liquid level inside the tank has considered approximately 90% of the total height. European and USA standards do not contain any suggestion for seismic analysis of the storage tanks' roof as stated by Pantusheva (2017). Besides, the tank is initially assumed to have no roof structure like previous studies as defined by Erkmen (2017), Ormeno et al. (2012), and

Phan et al. (2018). Since an unanchored liquid storage tank is considered, the main interests of this study is the buckling of the cylinder shell and the uplift of the base plate of the storage tank.

Table 4.1 Geometric parameters of unanchored steel storage tank and liquid

	Property	**Nominal value**	**Unit**
Tank	Radius of tank	27.432	m
	Height of tank	15.6	m
	Shell plate thickness	33, 29.5, 25.5, 21.5, 17.5, 14, 10, 8, 8, 10	mm
	Annular ring	L 100x100x10	mm
	Bottom plate thickness	8	mm
Liquid	Liquid level	14	m

Material properties of the unanchored steel storage tank taken from Phan et al. (2019a) are shown in Table 4.2. Also, the shell plasticity was modeled using the yield criterion of von Misses, an elastic-perfectly plastic behavior in the case of large base plate uplift, and steel yield stress of 235 MPa is taken from API (2007). The mass density of the liquid (crude oil) and tank are $\rho_L$and ρ, respectively. The modulus of elasticity and Poisson's ratio for the steel tank material are expressed as E and υ. In the explanation about damping in the study conducted by Tavano (2011) on storage tanks, it is necessary to perform rational studies and estimate the reasonable values to determine the damping rates determined by the standards. However, Habenberger (2015) stated that the damping in the impulsive component could be neglected in the analyses. Also, in the study conducted by Kwon (2015), it was observed that damping has neglected in the model with fluid-structure interaction. As a result, in this study, the damping effect is ignored.

Table 4.2 Material properties of unanchored steel storage tank and liquid

	Property	**Nominal value**	**Unit**
Tank	Density	7850	kg/m^3
	Young's modules	200,000	MPa
	Poisson's ratio	0.3	-
	Yield strength	235	MPa
Liquid	Density	900	kg/m^3

The finite element analysis software package ABAQUS is utilized to perform FEM analysis. Figure 4.1 shows the boundary conditions at the foundation in ABAQUS.

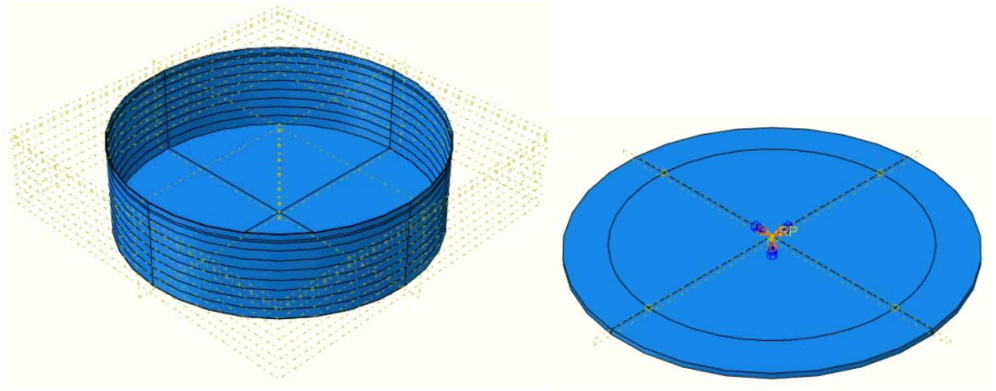

a. Storage tank b. Rigid foundation

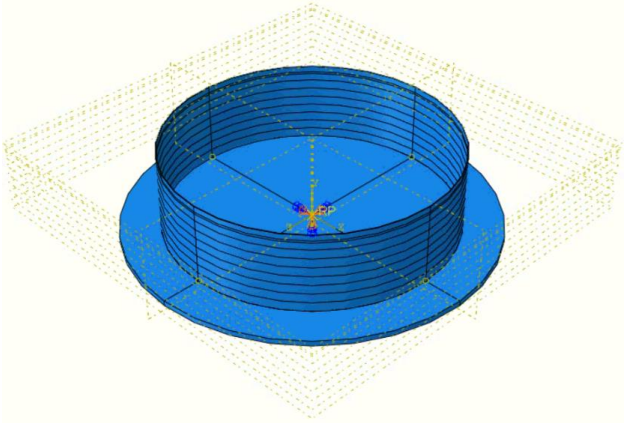

c. Tank-foundation system

Figure 4.1 Liquid storage tank modeled on ABAQUS

4.3 Fluid Structure Interaction

ABAQUS, the finite element modeling software with dynamic analysis capability, has been used to analyze the model of the liquid storage tank. Also, to consider the interaction in the model calculations, the finite element model utilizes the liquid effect, and the shell has been used. The fluid creates hydrostatic and hydrodynamic pressure on the storage tanks. Hydrostatic pressure is assigned to structure as a static load to the bottom and the wall of the storage tank via the following equation.

$$p_{hydro-static} = \rho_L g H_L \quad (4\text{-}1)$$

Moreover, the storage tanks have two different fluid parts under seismic loading, which are impulsive and convective components of liquid action. The impulsive part behaves like a rigid body, and the convective part has moved during analysis and creates

sloshing in tank. For the sake of application of hydrodynamic fluid pressure to structure, impulsive pressure to be considered during storage tank analysis, as shown in Figure 4.2 and Figure 4.3. The expression gives the rigid impulsive pressure variation at the tank wall:

$$p_i(\xi,\eta,\theta,t) = C_i(\xi,\eta)\rho_L H_L cos\theta A_g(t) \tag{4-2}$$

Where $C_i(\xi,\eta)$ is the impulsive pressure coefficient, ξ and η are the dimensionless coordinates, ρ_L is the unit weight of the liquid, H_L is the height of the liquid inside of the storage tank, θ is shown in Figure 4.2, and $A_g(t)$ is the ground acceleration. The impulsive pressure coefficient can be calculated as

$$C_i(\xi,\eta) = 2\sum_{i=0}^{\infty}\frac{(-1)^i}{I_1'\left(\frac{v_i}{\gamma}\right) * v_i^2}\cos(v_i\eta)I_1(\frac{v_i}{\gamma}\xi) \tag{4-3}$$

Where, $I_1(\cdot)$, $I_1'(\cdot)$ are the first order modified Bessel function and its derivative, respectively. The aspect ratio of the tank, γ, dimensionless coordinates ξ, and η could be defined as shown in the following expression.

$$\begin{cases} v_i = \dfrac{2i+1}{2}\pi \\ \xi = \dfrac{r}{R} \\ \eta = \dfrac{z}{H_L} \\ \gamma = \dfrac{H_L}{R} \end{cases} \tag{4-4}$$

Where r and z are the cylindrical coordinate system. The modified Bessel functions general equation is defined by the following equation

$$I_j(\Phi) = \left(\frac{\Phi}{2}\right)^j \sum_{k=0}^{\infty}\frac{\left(\frac{\Phi}{2}\right)^{2k}}{k!\,(j+k)!} \tag{4-5}$$

The Bessel function order of zero as shown following expression

$$I_0(\Phi) = \sum_{k=0}^{\infty} \frac{\left(\frac{\Phi}{2}\right)^{2k}}{k!^2} \tag{4-6}$$

The Bessel function order of 1 as shown following expression

$$I_1(\Phi) = \frac{\Phi}{2} \sum_{k=0}^{\infty} \frac{\left(\frac{\Phi}{2}\right)^{2k}}{k!\,(1+k)!} \tag{4-7}$$

The derivative of the first order Bessel function is shown at following expression

$$I_1'(\Phi) = \frac{dI_1(\Phi)}{d\Phi} = I_0(\Phi) - \frac{I_1(\Phi)}{\Phi} \tag{4-8}$$

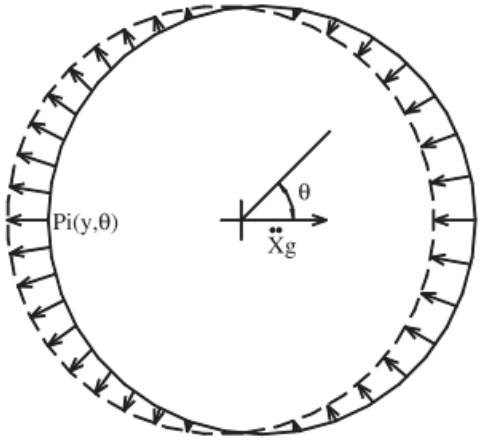

Figure 4.2 Circumferential impulsive pressure distribution (Virella et al., 2005)

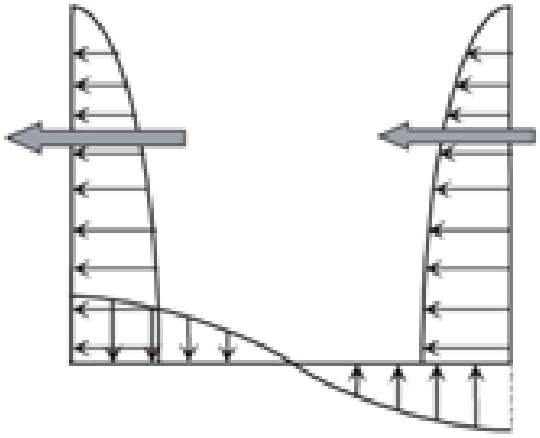

Figure 4.3 Impulsive pressure distribution along the wall and the base of the liquid storage tank (Jaiswal and Jain, 2005)

4.4 Soil Structure Interaction

The deformability of the soil is of considerably essential for the dynamic analysis of liquid storage tanks, and the response of the structure affects the configuration of the building. As explained by Karim (2008) “They found that for rigid tanks, soil deformability amplifies the response of tall tanks; however, broad tanks were found to behave as if they are supported by a rigid foundation.” Consideration of the foundation flexibility reduces the fundamental natural frequency and overall stiffness of the storage tank system. However, the unanchored cylindrical liquid storage tanks are generally assumed to lay on a rigid foundation.

The interaction of soil structure affects the period of impulsive mode. In this thesis, only soil-structure interaction is considered in FEA of an unanchored circular liquid storage tank. The interaction property is defined as 0.4 in relation to the friction between the base plate of the liquid storage tank and the rigid foundation, as defined by API (2007). In the analysis, the tank was assumed to rest on a circular rigid foundation. Both the rigid foundation and the tank model were investigated by using the finite element analysis.

4.5 Structural Modeling

ABAQUS is a computer-aided engineering software which is a suite for the finite element analysis. It includes ABAQUS/Standard, a general-purpose finite element

analyzer that employs an implicit integration scheme (traditional), and ABAQUS/Explicit, a special purpose finite element analyzer that employs explicit integration scheme to solve highly nonlinear systems with many complex constants under transient loads. The analysis modules are combined into ABAQUS/CAE environment to modeling, analyzing, visualization purposes.

ABAQUS/CAE divided into modules to define and analyze the system in a logical pattern. These modules are Part, Property, Assembly, Step, Interaction, Load, Mesh, Optimization, Job, Visualization, and Sketch modules. The model's geometric components are created in the Part module and geometric and material properties of each component's definition and assignment to parts made at the Property module. The Assembly interface in ABAQUS lets to create and modify the assembly of the model with composing the components created at the Part module. In the Step module analysis type, and the result types are specified. The Interaction module used to assign structure and rigid foundation interaction. The Load module is used to define loads and related boundary conditions of steps. The mesh module used to create meshes to make finite element analysis via proper mesh type.

The analyses are performed by using finite element analysis computer software ABAQUS. Figure 4.5 shows the structural configuration of the considered storage tank system, where the unanchored liquid storage tank rest on the rigid foundation, as shown in Figure 4.5 (a) and tank shell model shown in Figure 4.5 (b). The contact properties defined to assign interaction between the rigid foundation and the base plate of the liquid storage tank. The rigid foundation was modeled as a 4-node 3D bilinear rigid quadrilateral (R3D4) element. The storage tank's wall, and base modeled as a 4-node doubly curved thin or thick shell element, reduced integration, hourglass control, finite membrane strains (S4R). The loading of the tank is applied in two steps considering gravity, hydrostatic and hydrodynamic loads, as shown in Figure 4.4. In the first step, the hydrostatic and gravitational loads applied to the storage tank as quasi-static loading as shown in Figure 4.6 (a-b). In the second step, the impulsive hydrodynamic pressure assigned to the tank wall and base during time-history analyses, as shown in Figure 4.6 (c). The application of the impulsive pressure is the most complicated part of the modeling. The impulsive pressure component on the liquid storage tank's wall is assigned into two pieces, which are assigned to the +x and -x sides of the tank wall. The impulsive pressure direction during time history analysis is shown in Figure 4.4 (c) change with the ground motion excitation direction. The pressure assigned at the ABAQUS software with the creation of

an analytical field definition. The analytical model is generated based on the analytical definition, which has explained in the part 3 of Chapter 4. Therefore, a python programming language used to write a proper code to assign pressure at the wall and the base of the storage tank during analysis in ABAQUS. Also, the flowchart of the python code for impulsive pressure is shown in Figure 4.7.

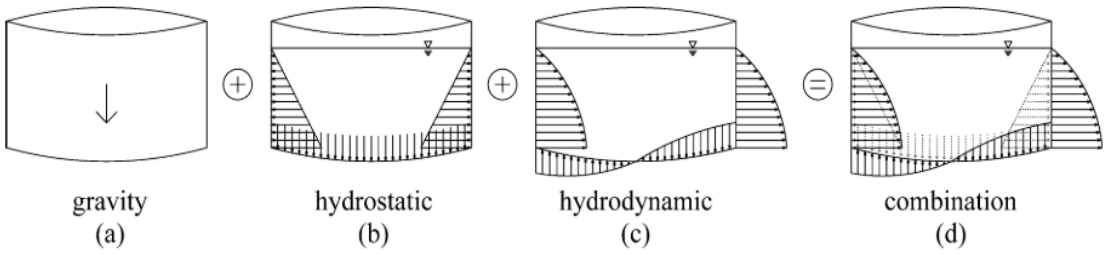

Figure 4.4 Loading steps: (a) gravity loads; (b) hydrostatic pressure; (c) hydrodynamic pressure; (d) combined actions (Bakalis, 2018)

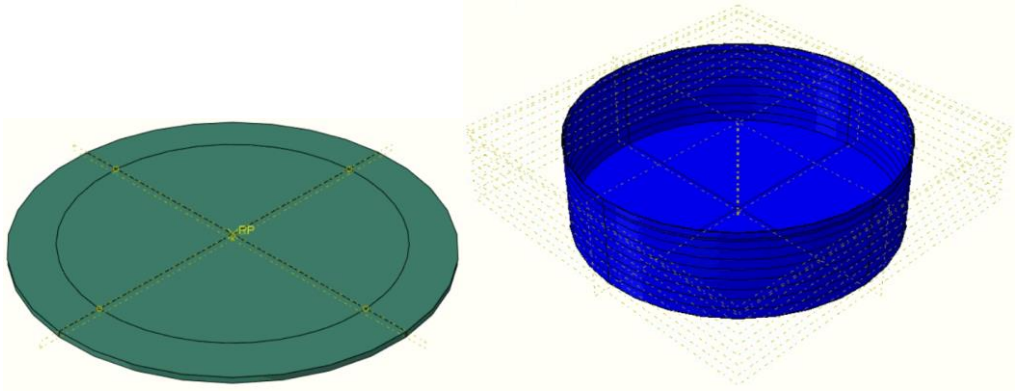

(a) (b)

Figure 4.5 The storage tank system (a) rigid foundation, (b) tank model

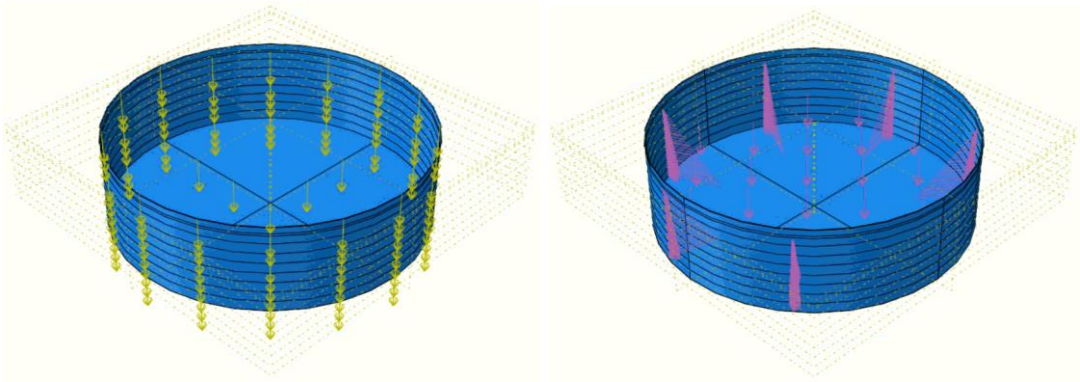

(a) (b)

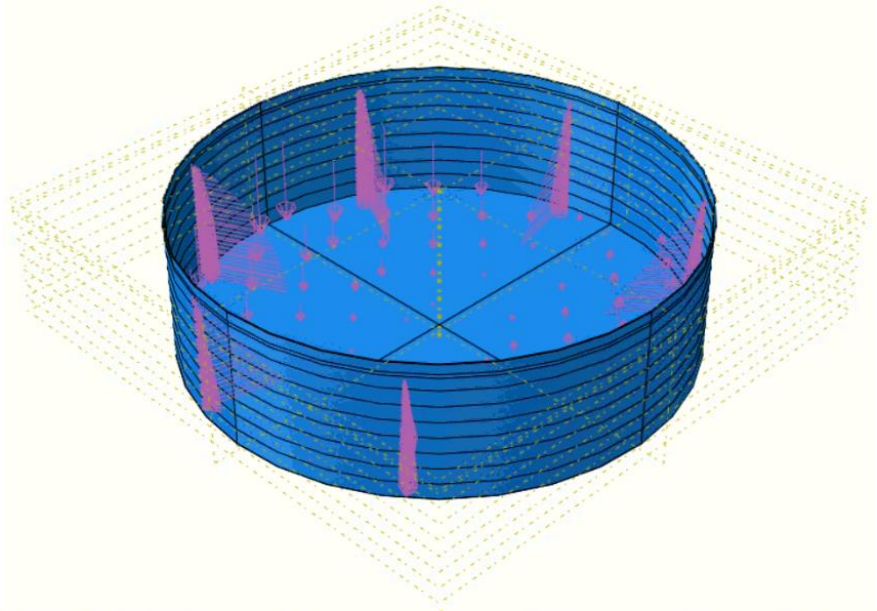

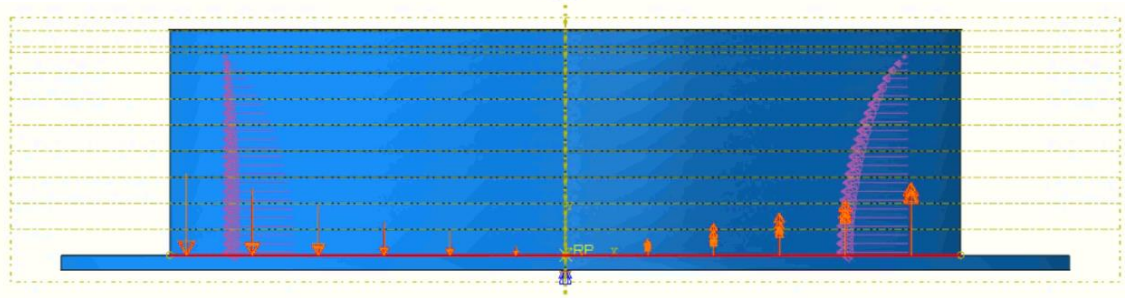

(c)

Figure 4.6 Loading steps for liquid storage tank: (a) gravitational loads, (b) hydrostatic liquid pressure, (c) hydrodynamic liquid pressure

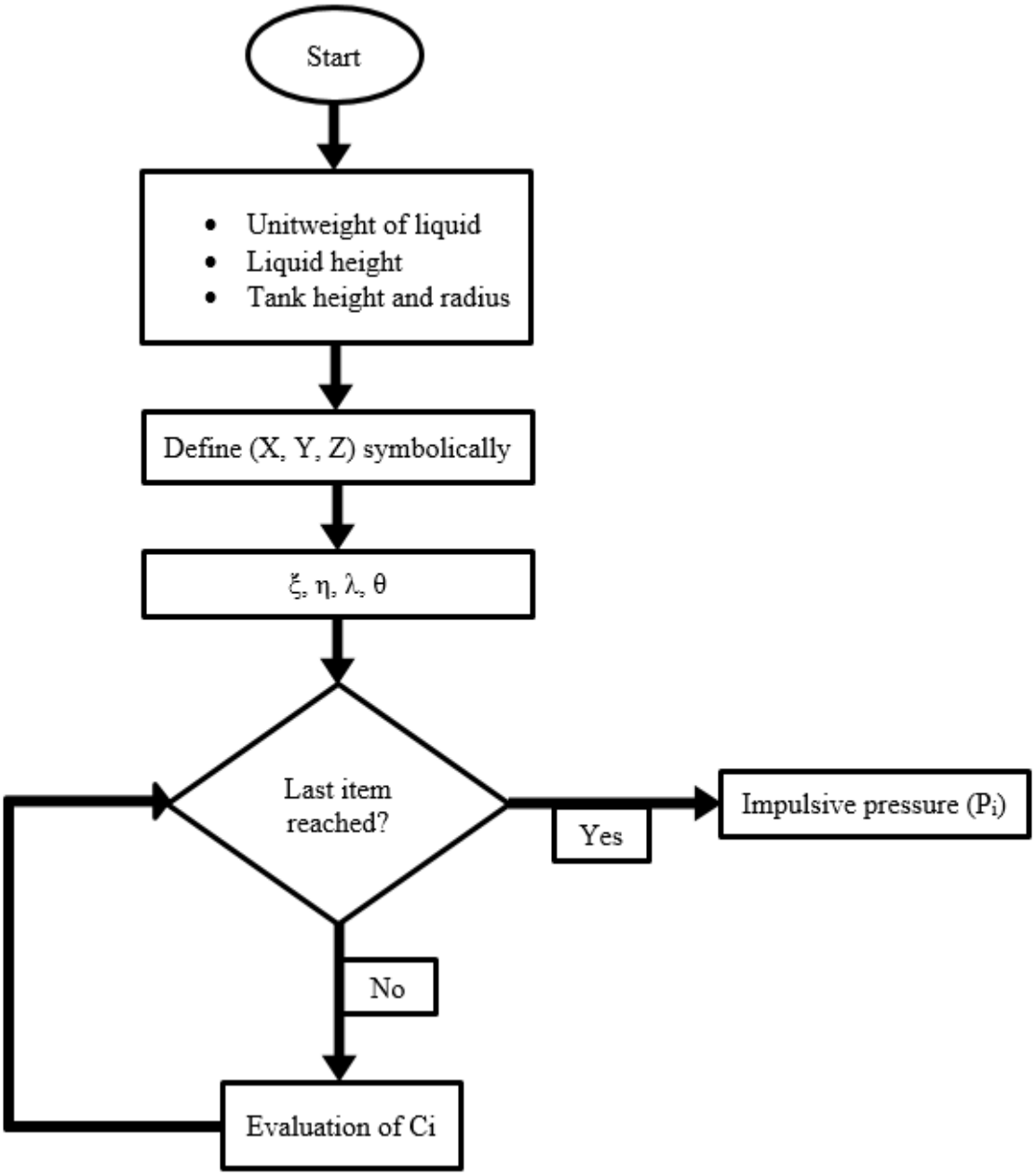

Figure 4.7 Flowchart to calculate impulsive pressure formulation at python

CHAPTER 5

INCREMENTAL DYNAMIC ANALYSIS

5.1 Introduction

In the Northridge earthquake (1994), damages were observed at liquid storage tanks and steel moment resistant frame connections. Therefore, a new analysis method was studied to analyze the structures for dynamic actions in detail. In early development stages, the Incremental Dynamic Analysis (IDA) approach was initially scaled to Dynamic Pushover and constructed as a way of estimating the relationship to the system's global failure. This approach had limits such as life safety to be reviewed. Subsequently, this approach was used as the basis for a number of standards for the assessment of the hazard level of the model. Besides, the liquid storage tanks have two other main non-linear structural analysis methods, which are the static pushover (SPO) and the endurance time (ET) method. In SPO, the fluid pressure increases with time and evaluate the base shear and base moment of the model. The SPO methodology in storage tanks is applied as distributed pressure on the shell. As described by Cortes et al. (2011), Sobhan et al. (2017) and Vathi (2014), when applying the SPO method, the pressure is applied perpendicular to the surface of the storage tank. Also, the central height of impulsive pressure coincides with the central height of SPO pressure. Moreover, the ET is a dynamic pushover procedure for seismic assessment of structures. ET is a procedure with a single response history to predict the structural response at different equivalent seismic intensity levels. The basic concepts of the ET were published by Estekanchi et al. (2004) and the ET method applied to anchored liquid storage tanks by Alembagheri & Estekanchi (2011). Consequently, IDA, SPO, and ET are important methods used for structural performance calculation. However, since IDA consists of various earthquake data and a variety of intensity measure (IM) values, it is an essential method in terms of calculating the response of the model. Therefore, the incremental dynamic analysis principle has received broad attention in the earthquake research community. In light of the information provided, the seismic assessment process consists of two general phases:

1. Defining the geometric layout of the appropriate load-resistant liquid storage tank system, as shown in section 4:

2. The performance evaluation of either linear or non-linear, static, or dynamic analysis of the resulting design is presented in detail in this chapter.

In this study, the seismic performance of the liquid storage tanks considered evaluating with regard to the Performance-Based Earthquake Engineering (PBEE) concepts. As explained by Vamvatsikos (2002), one of the most important PBEE tools is the Incremental Dynamic Analysis (IDA) method, which involves nonlinear dynamic analysis under seismic loading, each ground motion scaled to a proper IM to evaluate the performance of the model. Also, limit state and demands for IDA are calculated by applying nonlinear time history analysis to the storage tank model with a large number of scaled earthquake ground motion data. A great deal of effort should be made to create comprehensive calculations of IDA with a wide range of nonlinear dynamic analyses. Despite this, ID has proven to be the most effective method of use in probabilistic vulnerability and risk assessments. With the new earthquake data generated by multiplying the earthquake ground motion selected for IDA with a specific coefficient, their analysis is repeated until they reach the limit state. The accuracy of the results obtained with IDA is also related to the number of earthquake ground motions used in the analyzes. Besides, the IDA figure shows the structural response or damage measure (DM) versus the typical scalar IM value by performing appropriate post-processing.

In this chapter, the procedure and timeline of the IDA are detailed in part 5.2. Part 5.3-5.4 explain the procedure from selection to scaling of the ground motion data with proper software, code and sites. Part 5.5 explains the nonlinear dynamic analysis to perform the IDA. Finally, part 5.6 shows the results of the IDA with a proper figure.

5.2 Procedure and Timeline

IDA is a comprehensive computational method to evaluate structural response under earthquake excitation. Also, IDA is based on variable nonlinear dynamic analysis of the structural model under scaled multiple ground motion excitation. It has been developed for the estimation of seismic risk assessment of a structural model. IDA can be considered as the dynamic equivalent of the static pushover analysis. To evaluate the performance of a model, IDA needs some steps, which are;

- A suitable nonlinear structural model has to be created as explained in Chapter 4, and a set of records have to be collected, as choose in part 5.3.

- The level of scaling has to be selected with respect to the initial control analysis as clearly defined in part 5.4, the dynamic analysis is carried out and the results determined with respect to considered failure criteria.

Subjects such as the number of runs, algorithms used for scaling-level selection, and potential approximations used for probabilistic calculations are discussed in this chapter showing their effect on the accuracy of PBEE.

The selection of the IM is one of the main components of the IDA. IDA involves conducting a number of non-linear dynamic analyses to assess structural response under the context of scaled ground motion excitation, as shown in Figure 5.1. Possible choices for IM are linearly or nonlinearly associated with the intensity and amplitude of recorded ground motion data. The IM is appropriate to the production of the seismic hazard analysis and for the creation of appropriate seismic hazard maps. Potential IM options include peak ground acceleration (PGA), peak ground velocity (PGV), and spectral acceleration. Many research suggest that the PGA is one of the most prominent IMs for the seismic assessment of liquid storage tanks.

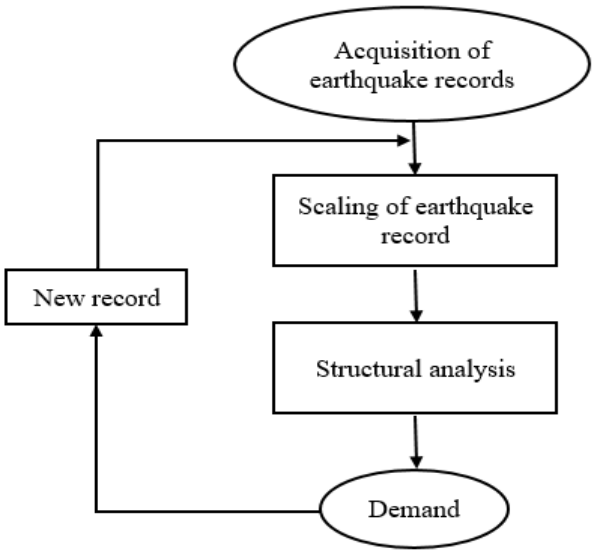

Figure 5.1 Flow chart for IDA

IDA is an important method in terms of reflecting more or less extreme earthquakes by scaling the earthquake records those reported at the site. The rate of scaling is correctly chosen to force the structure through an elastic, inelastic and dynamic destabilizing behaviour of the system. In general, the structure is collapsing in the dynamic destabilization of the system. IDA is challenging to implement, and its accuracy

is often directly related to the step length of IM. Generally, the researchers use a small set of three to seven ground motion data in order to obtain an estimate of the response in the considered field.

The simplest way to determine IDA is to define the increment of IM from beginning to collapse. IDA consists of a combination of nonlinear dynamic analysis' results and shows the corresponding set of points on the IM-demand curve. The algorithm is needed to have a defined step length, approximate final level IM, and approximate analyses time needed to complete the IDA philosophy. Even if, the analyses made by a selected and scaled ground motion data as explained respectively in part 5.3 - 5.4, the step length of the IM could be too large or small. Also, one of the main definition of the IDA philosophy is to define the boundary of damage.

IDA describes multiple perspectives for the dynamic response of the structure and presents a range of possible responses by considering a sufficient number of ground motion data. So we can generate IDA curves of the structural response, as evaluated by damage measure (DM), (e.g., elephant foot buckling, base plate plastic rotation), versus IM. On the other hand, the evaluated values interpolated to summarize the overall record for the development of DM versus IM distribution. An effective post-processing for the assessment of the liquid storage tanks can be present by IDA curve, which arises from a scalar IM versus a calculated engineering demand parameter (EDP).

IDA is determined from the maximum non-linear response of the structure under one or more scaled ground motion records. The EDP could be a structural, nonstructural or content response. The general failure criteria considerations for assessment of liquid storage tanks are based on wall compressive meridional stress, base plate plastic rotation, and so on.

Instead of the simplicity of the incremental dynamic analysis, evaluation of the IDA is potentially intensive. The intensity of the grid on the curve intent to take into consideration each IM to evaluate more accurate structural response. As a result of the information obtained from a single IDA response, the IM value of the next record for multiple IDA calculations is determined. This lead in defining IM step length and define boundary to consider possible failure IM. Consequently, the multi-record IDA is considered in this study for the selected unanchored steel circular liquid storage tank.

5.3 Ground Motion Selection

The selection and the scaling of the ground motion data is one of the essential parts of the application of IDA in earthquake engineering. According to the methodology proposed by FEMA (2009) for the collapse assessment within the dynamic analysis is made by using the ground motion recordset consists of two groups, which are near-field recordset and far-field recordset. The far-field recordset consists of 22 earthquake ground motion data taken from locations located at a distance of at least 10 km from fault rupture. Also, the near-field record set consists of 28 earthquake data taken from locations within 10 km of the fault rupture. In this study, 22 pairs of far-field records set specified by FEMA (2009) are used for IDA calculations. However, as explained in by FEMA (2009), the vertical component of earthquake record is not of primary importance for the collapse assessment, nor it is not included in the application of nonlinear analysis.

There are two more commonly used sites by researchers and professionals to collect ground motion data, which are the Pacific Earthquake Engineering Research Center (PEER) and COSMOS Virtual Data Center. The web-based PEER ground motion database provides tools for searching, selecting and downloading ground motion data. Besides, the COSMOS Virtual Data Center is a public, web-based search engine for accessing worldwide earthquake strong ground motion data. In this study, both PEER and COSMOS websites used to download the selected far-field ground motion recordset with respect to FEMA (2009) Table A.4A at Appendix A, as shown in Table 5.1.

Table 5.1 Far-field ground motions data set (FEMA, 2009

ID	Earthquake			Recording Station	Recorded Motions
No.	M	Year	Name	Name	$PGA_{max}(g)$
1	6.7	1994	Northridge	Beverly Hills - Mulhol	0.49
2	6.7	1994	Northridge	Canyon Country-WLC	0.47
3	7.1	1999	Duzce, Turkey	Bolu	0.81
4	7.1	1999	Hector Mine	Hector	0.33
5	6.5	1979	Imperial Valley	Delta	0.35
6	6.5	1979	Imperial Valley	El Centro Array #11	0.38
7	6.9	1995	Kobe, Japan	Nishi-Akashi	0.48
8	6.9	1995	Kobe, Japan	Shin-Osaka	0.23
9	7.5	1999	Kocaeli, Turkey	Duzce	0.36
10	7.5	1999	Kocaeli, Turkey	Arcelik	0.21
11	7.3	1992	Landers	Yermo Fire Station	0.24
12	7.3	1992	Landers	Coolwater	0.42
13	6.9	1989	Loma Prieta	Capitola	0.51
14	6.9	1989	Loma Prieta	Gilroy Array #3	0.56
15	7.4	1990	Manjil, Iran	Abbar	0.51
16	6.5	1987	Superstition Hills	El Centro Imp. Co.	0.36
17	6.5	1987	Superstition Hills	Poe Road (temp)	0.51
18	7.0	1992	Cape Mendocino	Rio Dell Overpass	0.55
19	7.6	1999	Chi-Chi, Taiwan	CHY101	0.40
20	7.6	1999	Chi-Chi, Taiwan	TCU045	0.51
21	6.6	1971	San Fernando	LA - Hollywood Stor	0.22
22	6.5	1976	Friuli, Italy	Tolmezzo	0.36

5.4 Ground Motion Scaling Procedure

Many methods for scaling ground motion data, as shown in Table 5.2 have been developed for nonlinear analysis of liquid storage tanks. For example, $S_a(T_c)$ is one of the most important intensity measures (IMs) for the development of sloshing failure. For the sake of the calculations, peak ground acceleration (PGA) is used as an IM.

Moreover, the ground motion record scaling involves two steps, which are normalization and scaling. Ground motion records in each set are normalized with respect to the peak ground acceleration of individual ground motion. The importance of this step is the elimination of unwarranted variability between records. The unwarranted variability is the effect of the earthquake magnitude, source distance, type of source and field conditions.

Table 5.2 Type of IMs for seismic assessment of liquid storage tanks (Bakalis, 2018)

Intensity Measures*		
Scalar		Abbreviation
PGA		IM_{s1}
$S_a(T_i)$		IM_{s2}
$S_a(T_c)$		IM_{s3}
$\sqrt{S_a(T_i) \cdot S_a(T_c)}$		IM_{s4}
$\sqrt{S_a(T_i) \cdot S_a(1.5T_i)}$		IM_{s5}
$\sqrt{PGA \cdot S_a(T_c)}$		IM_{s6}
$AvgS_a = \left[\prod_{j=1}^{m} S_a(T_{Rj})\right]^{1/m}$	$0.1s \le T_{Rj} \le 0.6s\ (\approx 2.7T_i)$	IM_{s7-1}
	$0.1s \le T_{Rj} \le 1.0s\ (\approx 4.5T_i)$	IM_{s7-2}
	$0.1s \le T_{Rj} \le 1.5s\ (\approx 6.8T_i)$	IM_{s7-3}
Vector		
$\{PGA, S_a(T_c)\}, or\ equivalently$	$\{PGA, S_a(T_c)/PGA\}$	IM_{v1}
$\{S_a(T_i), S_a(T_c)\}, or\ equivalently$	$\{S_a(T_i), S_a(T_c)/S_a(T_i)\}$	IM_{v2}

* All spectral ordinates refer to the geometric mean of the longitudinal and transverse earthquake recordings

Normalized ground motions are collectively scaled to a specific ground motion intensity (FEMA, 2009). The PGA scaling being in the conservative approach yielded more realistic ground motion characteristics in terms of calculated peak ground accelerations on the ground surface. The PGA scaling technique consists of multiplying the acceleration time history by a scale factor. After the multiplication of the ground motion data with the appropriate scale factor, the target ground motion data is obtained with the target PGA.

To get different PGA, ground motion data scaling need to be applied to the selected set. There are two different scaling procedures can be used. Each ground motion data can be normalized with respect to peak ground acceleration of each sample, or each ground motion data can be normalized with respect to mean of the peak ground acceleration of the all ground motion records explained by Cimellaro et al. (2006). These two options are described, step by step below.

First case normalization and scaling procedure:

1. Evaluate the PGA of each ground motion set to define the normalization factor.

$$PGA_i = MAX\left(\left|\ddot{X}_{0i}(t)\right|\right) \tag{5-1}$$

Where the total number of ground motions considered in this study is 22, and i change in range of the number of ground motion, $\ddot{X}_{0i}(t)$ is the peak ground acceleration of the ground motion record.

2. Normalize each horizontal direction ground motion data with respect to peak ground acceleration of each sample evaluated at previous step.

$$\ddot{X}_{0i}(t) = \frac{\tilde{\ddot{X}}_{0i}(t)}{PGA_i} \tag{5-2}$$

Where $\tilde{\ddot{X}}_{0i}(t)$ is ground motion data obtained with the accelerometer, PGA_i is the absolute PGA of the consider ground motion data and $\ddot{X}_{0i}(t)$ is the normalized ground motion data of selected earthquake record.

3. Each ground motion data selected is scaled to achieve the purpose of this study. Each ground motion in the dataset is multiplied by a scale factor calculated in the previous step.

Second case normalization and scaling procedure:

1. Evaluate the PGA of each ground motion data, as explained by Equation (5-1) in the first step of the first case.
2. Compute mean of the evaluated PGA of selected ground motion data set as the following expression:

$$\overline{PGA} = MEAN(PGA) \tag{5-3}$$

Where, $\overline{PGA}$ is the mean PGA of the selected accelerogram records.

3. Normalize each ground motion data with the evaluated mean of the PGA of all selected ground motion data.

$$\ddot{X}_{0i}(t) = \frac{\tilde{\ddot{X}}_{0i}(t)}{\overline{PGA}} \tag{5-4}$$

4. For scaling the selected ground motion data, each data in the set is multiplied by the scale factor according to single IDA.

Both of the techniques for the scaling of the ground motion data give approximately the same results, as explained and calculated by Cimellaro et al. (2006). Therefore, in this study first case used to scale ground motion set and to normalize and scale ground motion data downloaded from PEER and COSMOS data centre, the python programming language used to read and write accelerogram records from text to excel file.

5.5 Nonlinear Dynamic Analysis

In the nonlinear dynamic analysis of structures, the nonlinear geometric and material properties of the model are considered. The nonlinear dynamic analysis methodology of the model shall be in accordance set out by FEMA (1997). The nonlinear dynamic analysis uses a combination of ground motion data and a detailed model, so the results are relatively accurate, which is the most comprehensive approach to determine the response of the structure with uncommon configuration. In the nonlinear seismic analysis, inertial seismic forces, distribution of inertial seismic forces over the height of the model, and internal reactions are determined. Also, the evaluated response could be very sensitive to the properties of assigned ground motion data. Therefore, quite accurate results are obtained in terms of performance evaluation of the model by using a variety of ground motion data.

The seismic response is related to the intensity or severity of the ground motion excitation. Using multiple earthquake records is an effective way to determine the response of the model comprehensively, which has brought about the emergence of methods such as the IDA. The modelling approaches, acceptance criteria of the IDA are based on nonlinear dynamic analysis. The earthquake shaking should be characterized with respect to FEMA (1997) to achieve the expected performance level. Three pairs of ground motion records shall be used as a minimum number of considered seismic data.

In the three-dimensional nonlinear dynamic analysis, the structural response is a complex phenomenon. However, the nonlinear dynamic analysis of structure almost entirely represents the dynamic response of the model, as shown in Figure 5.2. The development of computer technology decreases the analysis time; therefore, the nonlinear dynamic or time-history analysis have more extensive usage. Nonlinear dynamic analysis was performed with the input of ground motions from the far-field recordset to evaluate

IDA. IDA is obtained by applying many earthquakes ground motion data with increasing intensity to the model until the collapse occurs in the time-history analysis. This methodology is applied with a sufficient number of earthquake ground motion records to determine the median collapse capacity as well as the variability between records.

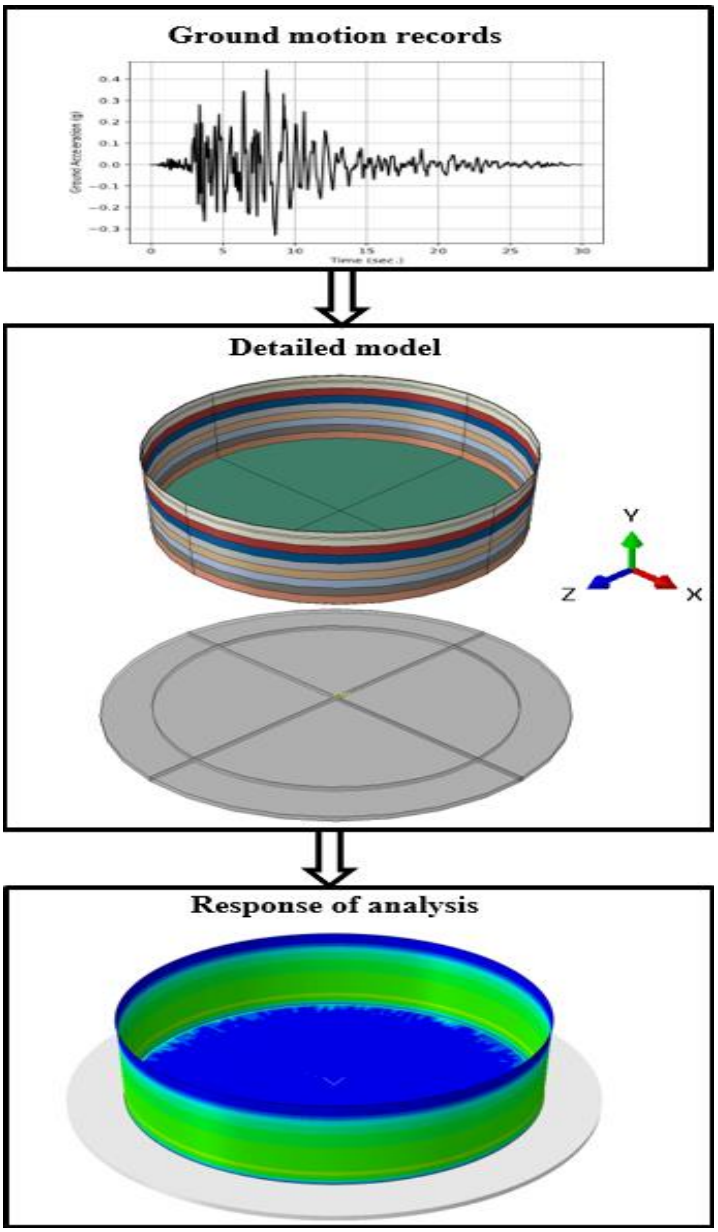

Figure 5.2 Flow chart for the nonlinear dynamic analysis process of an unanchored circular liquid storage tank model

For the response evaluation of the three-dimensional finite element model, nonlinear time history analyses assessed with ABAQUS. Also, the 3D finite element model is the accurate physical representation of the system to evaluate reliable results.

Following the FEMA (2009) methodology, each scaled ground motion (each component of the 22 pairs of ground motion records) is rescaled with increasing intensity to the IM at which the model reaches a collapse limit state. Minimum five analyzes should be performed for each record, and a total of 132 nonlinear response history analyzes should be performed for each index archetype model. The numerical model considers the nonlinearity at the material and geometrical representation, therefore, evaluated internal forces could be more realistic.

5.6 Result of Analyses

The main components of the IDA are IM and DM selection, and post-processing of the analysis. The selection of the DMs relates to the selected failure criteria and structural geometry as shown in part 3.1 with Eq. (3-1) for EFB and part 3.5 with Eq. (3-8) for base plate and wall-to-base connection rupture . The objective is to focus on structural instability in relation to the specified levels of performance. After the selection of IM and DM, IDA should be presented and plotted in a meaningful way as it has many implications.

To apply the IDA methodology for this study, analyzes were conducted up to approximately twice the IM value, in which the median collapse capacity occurred, for both EFB and base plate and wall-to-base connection rupture. Therefore, the analysis was conducted with linearly increasing peak ground acceleration from 0.05 g to 0.50 g for EFB and 0.1 g to 1.0 g for the base plate and wall-to-base connection rupture. Figure 5.3 and Figure 5.4 show the direct result of structural response in a meaningful plot after post-processing. Even then, the IM tends to be out of balance in the distribution. Besides, in the low IM levels, the responses are close to each other, while those responses at higher IM levels are scattered, and the number of collapses is increasing dramatically.

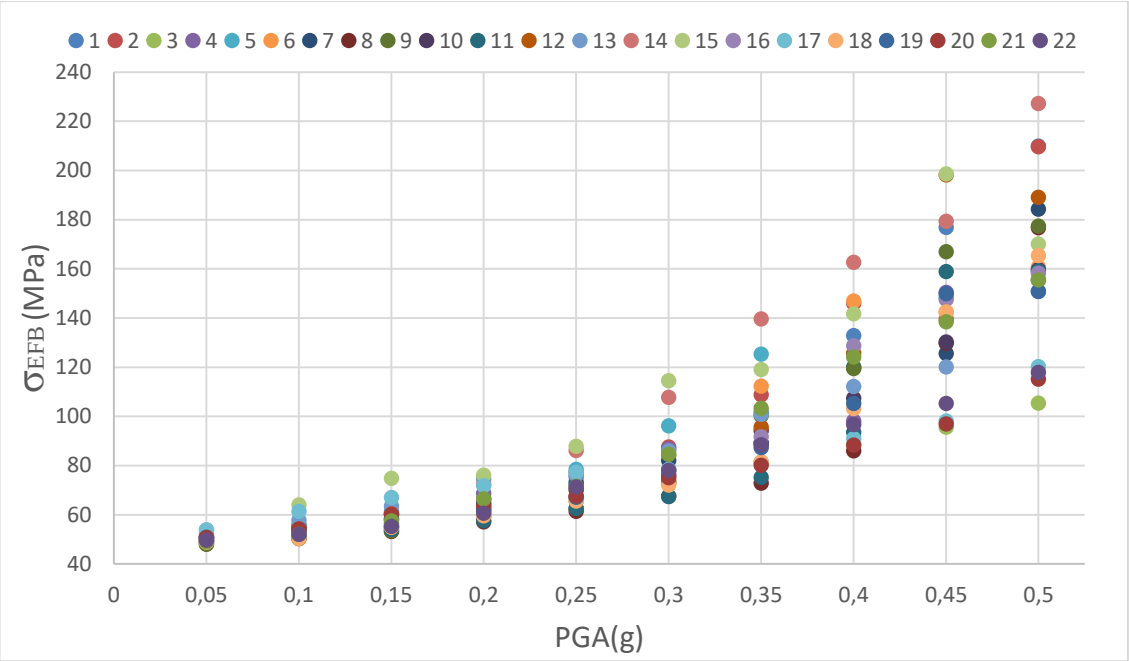

Figure 5.3 The maximum compressive meridional stress vs peak ground acceleration

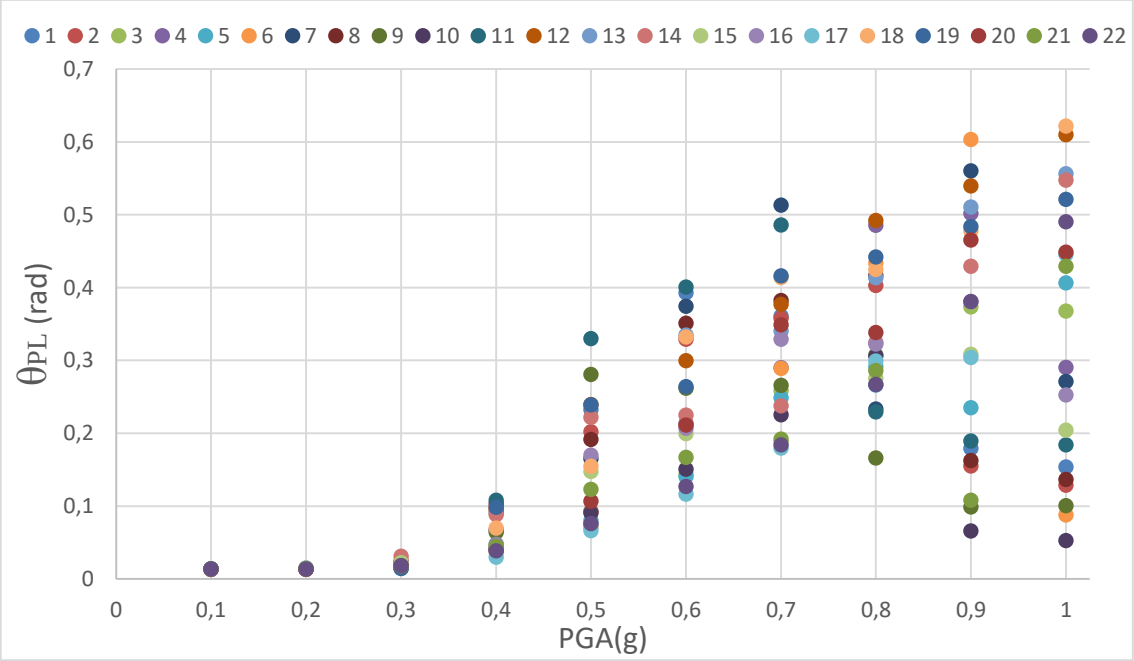

Figure 5.4 The plastic rotation vs peak ground acceleration

CHAPTER 6

SEISMIC FRAGILITY ANALYSES

6.1 Introduction

This section provides a detailed explanation for the analysis of the seismic fragility of unanchored circular liquid storage tanks. The formulation of the fragility analysis is essential for the calculation of the seismic performance of liquid-containing structures. Also, the fragility analysis is one of the most appropriate analytical techniques for assessing loss of content and damage parameters.

Most of the time, the assessment of the fragility curve at storage tanks is based on PGA as an IM. In terms of analysis, the IM versus DM figure shows the response of the model for IDA to determine the fragility curve. In order to characterize the damage at the considered system, the damage states are considered as defined in Hazards United States (HAZUS). Besides, the damage states of the American Lifelines Alliance (ALA) also considered the failure criteria set out in Chapter 3 in the evaluations. The seismic performance of the unanchored circular liquid storage tank with fragility analysis under the defined damage conditions in HAZUS and ALA is evaluated in light of this information.

This section outlines the procedure for the development of the fragility curve and the definition of the damage states concerning possible failure criteria. Finally, the fragility curves have evaluated show the performance of the model at different PGAs.

6.2 Fragility Curve Development Procedure

One of the most critical aspects of the seismic fragility curves is to understand the performance of the model against seismic excitation. In this way, different ground motion IMs are used to understand the exceeding probability or entering a damage state, as shown in Table 5.2.

Repeated nonlinear dynamic analysis for the structural vulnerability assessment process has led to the development of fragility curves for various ground motion intensity

quantities. The analytically derived fragility curve is based on the IM-based conditional probability. These curves show the potential of a model in a probabilistic way for IM perceived ground motion. This provides a continuous correlation between IM and the failure probability. Also, the nonlinear analysis of the structural model makes it possible to assess the probability of damage states explained in Table 6.1 and shown in Figure 6.1. Each level of damage is characterized by the damage caused to the structural system, the non-structural system, and the loss of content. During any ground motion, the uncertainty of the structural model is shown by fragility curves.

Table 6.1 Damage states (HAZUS, 2010

Damage State	Description
DS1	No damage
DS2	Slight damage
DS3	Moderate damage
DS4	Extensive damage
DS5	Complete (collapse) damage

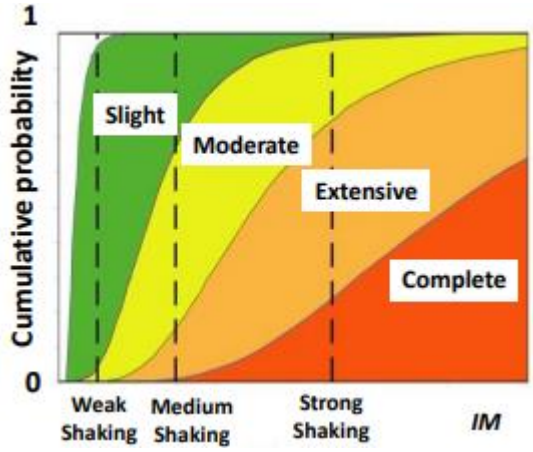

Figure 6.1 Damage states of liquid storage tank in a fragility curve

There are different types of distributions used for fragility analysis, which are normal (Gaussian), lognormal, and uniform distribution. Besides, lognormal cumulative distribution is widely used for fragility curves because its properties that are simplicity, precedent, information-theory reasons, often fit data. When a variable is distributed log-normally, it is natural logarithm normally distributed as explained by Porter (2020). This means that it must have a positive real value, and the probability that it will be zero or negative is zero.

Fragility function is an indicator of the probability of seismic demand that may occur in a structure that exceeds the boundary capacity for different IM values. If the structural capacity and response are expected log-normally distributed, the probability of failure of the model calculated by cumulative lognormal function for any damage state. The power function of the mean demand could be specified as in the equation below to calculate the average demand as defined by Nielson & DesRoches (2019):

$$D_m = a(IM)^b \tag{6-1}$$

Where a and b are the constant values evaluated from the linear regressions based on d_i and IM_i values estimated from nonlinear time-history analyzes of the liquid storage tank. In the field of seismic demand regression analysis, the dispersion of the demand ($\beta_{d|IM}$) is based on d_i and IM_i approximated by Mangalathu et al. (2018), as explained following equation:

$$\beta_{d|IM} \cong \sqrt{\frac{\sum_{i=1}^{N}[\ln d_i - \ln aIM_i^b]^2}{N-2}} \tag{6-2}$$

Where N is the number of nonlinear time-history analyses, d_i is the demand evaluated by each nonlinear time-history analyses, and IM_i is the PGA of each ground motion of time-history analyses. The probability of failure at a defined limit state (LS) based on IM at the engineering demand parameter (D_{EDP}) by Phan et al. (2019a) is shown in the following equation with the cumulative distribution function given as:

$$P[D_{EDP} > LS|IM] = 1 - \Phi\left(\frac{\ln LS_m - \ln D_m}{\sqrt{\beta_{d|IM}^2 + \beta_{LS}^2}}\right) \tag{6-3}$$

Where $\Phi(\cdot)$ is the standard normal cumulative distribution function, LS_m is the mean of the structural limit state, D_m is the mean of the demand, $\beta_{d|IM}$ is the dispersion of the demand conditioned on the IM, and β_{LS} is the dispersion of the structural limit state. β_{LS} is used to consider uncertainty of the limit state of selected failure criteria. β_{LS} is

used by Phan et al. (2019a) equal to 0.5 with respect to FEMA (2018), is assumed limit state dispersion for EFB and base plate and wall-to-base connection rupture.

As a result, the procedure of the fragility curve for liquid storage tanks from the selection of ground motions to plotting fragility curve explained with details above. The steps of the methodology to develop the fragility curve of selected failure criteria are described as a flow chart in Figure 6.2.

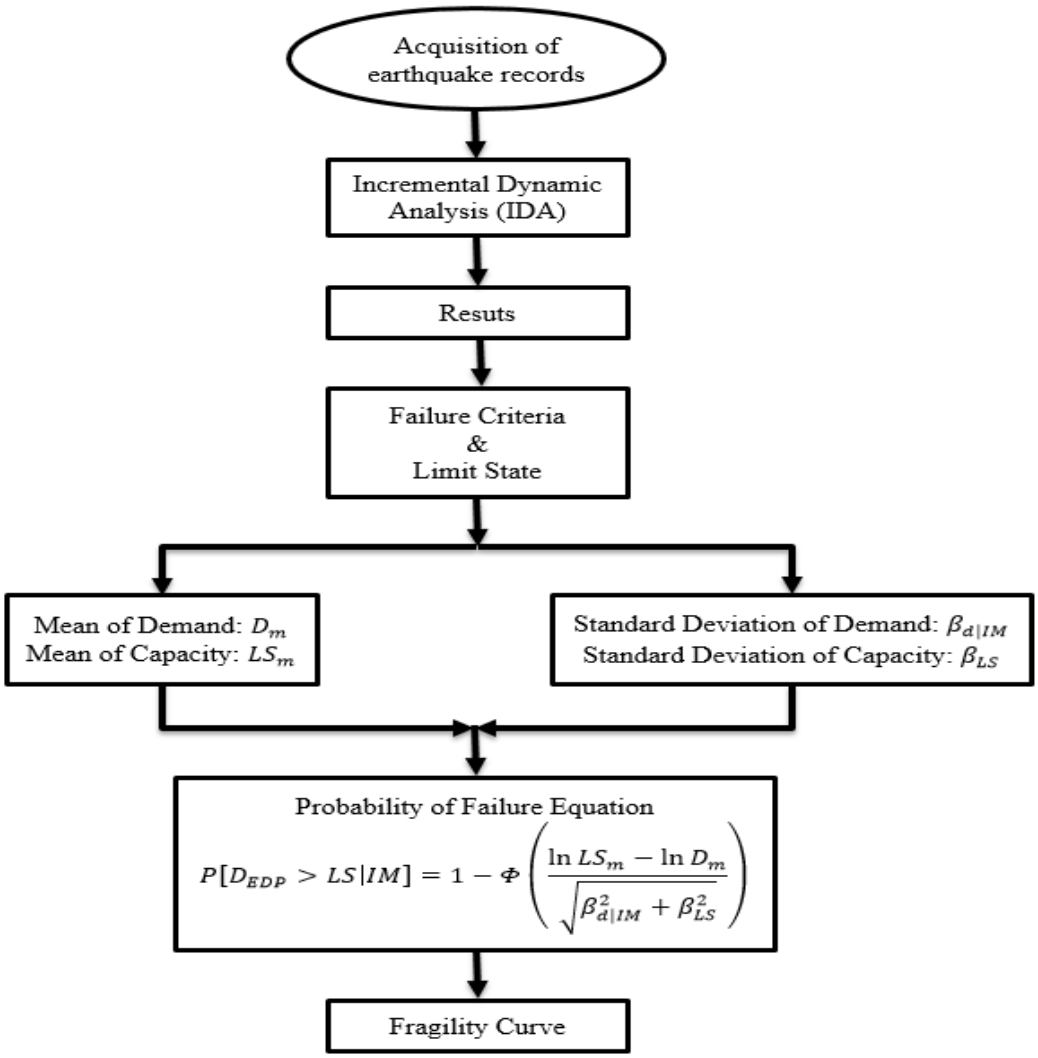

Figure 6.2 Fragility curve development flow chart

6.3 Definition of Damage States

In terms of failure defined criteria, liquid storage tanks consist of five damage states, as provided in Table 6.1. The damage state definition of engineering structures is defined as in HAZUS (2010). Also, the damage states defined in this part of the thesis are

described in ALA (2001) and HAZUS (2014). HAZUS contains general engineering structures' damage states. However, ALA derived these failure criteria for liquid storage tanks.

Generally, when the damage state increase, the failure severity in the structure increases as well. However, according to the statement made by D'Amico et al. (2018), the severity of the DS2 does not increase as in other damage states. The DS1 is defined by the minor damage to the top portion of the liquid storage tanks, as well as the yielding of anchors that occur because of the overturning moment. In the DS2, moderate rotation of the base plate, sloshing damage to the upper part of the storage tank, and anchor bolt failure shall observe without loss of content. The loss of content, extensive rotation at the base of a storage tank, EFB failure with no leakage, and piping system damage fits the content of the DS3. DS4 observe the EFB with loss of content (leakage), shell-base plate junction failure. The DS5 is complete damage or total failure of the liquid storage tanks. The above-explained failure criteria related to damage state of the liquid storage tanks are defined in Table 6.2 and shown in Figure 6.3. In this state, the observed damage types are loss of content, extensive EFB, tank collapse, an extensive damage to shell-base plate junction, and overturning.

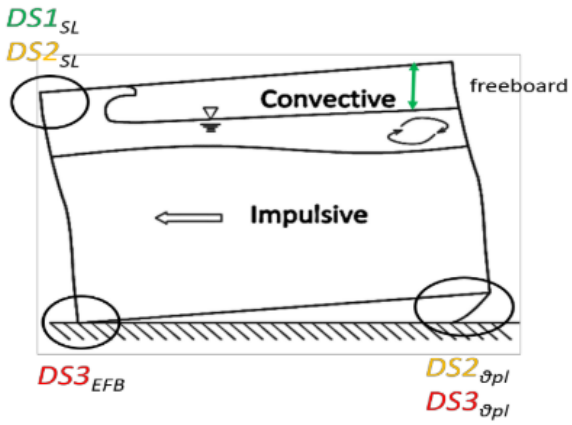

Figure 6.3 Damage states of the unanchored liquid storage tanks in a global and a local objective (Bakalis et al., 2015a)

Table 6.2 Damage state classification for liquid storage tanks (Bakalis, 2018)

	Failure Mode	DS (1)	DS (2)	DS (3)	DS (4)	DS (5)	References
Anchored	Sloshing (d)	$d > d_f$	$d > 1.4 \times d_f$				(API, 2007)
	Anchorage (δ)	$\delta > \delta_y$	$\delta > \delta_u$				Engineering Judgement
	Base plate plastic rotation (θ_{pl})		$\theta_{pl} > 0.2$ rad	$\theta_{pl} > 0.4$ rad			(CEN, 2006) (Cortes et al., 2012)
	EFB			$\sigma > \sigma_{EFB}$			(CEN, 2006)
Unanchored	Sloshing (d)	$d > d_f$	$d > 1.4 \times d_f$				(API, 2007)
	Base plate plastic rotation (θ_{pl})		$\theta_{pl} > 0.2$ rad	$\theta_{pl} > 0.4$ rad			(CEN, 2006) (Cortes et al., 2012)
	EFB			$\sigma > \sigma_{EFB}$			(CEN, 2006)

Where d is the sloshing wave height, and d_f is the freeboard that is available for sloshing, δ is an anchor bolt deformation, δ_y is the anchor bolt yield. Moreover, δ_u is the anchor bolt fracture deformation; θ_{pl} is the base plate plastic rotation of a storage tank. σ_m is the tank wall meridional stress level, and σ_{EFB} is the elephant's foot buckling stress limit.

Consequently, the development of the seismic fragility curves considers defined damage states for evaluating the model performance. Selected failure criteria could show different responses to different damage states. For example, EFB could cause to loss of the content after DS3.

6.4 Fragility Curve Results

Increasing the earthquake performance of the buildings is critical to reducing the total loss caused by the earthquake. Therefore, structural performance classes are determined by using fragility curves frequently in performance-based earthquake engineering (PBEE). The calculation of performance is expressed depending on the formulation as shown in Eq. (6-3). This formulation includes the effect of seismic intensity on demand and its dependence on capacity. It concludes the probability of failure and its dependence on IM in a well-defined fragility curve.

As the fragility curves play a critical role in structural performance calculations, accurate estimation of the seismic fragility of a structure is essential. Therefore, the focus

of has on the development of IDA-based vulnerability curves, as explained in previous sections. Also, the applicability of IDA for liquid storage tanks enables a more detailed performance calculation by creating the finite element analysis model detailly. The response of the IDA shows the IM versus demand distribution of the selected model as can be seen in Figure 5.3 and Figure 5.4. Also, by rising the earthquake records' number, the margin of error has further reduced and make results more accurate.

The nonlinear time history analysis of the liquid storage tank has performed to demonstrate the fragility curves depending on the damage state of selected failure criteria. Also, unlike well-studied structural systems (e.g., Moment-resistant frames) where increased seismic intensity result in higher damage states, the progression of the failure in the liquid storage tanks is not sequential (using the considered limit state capacities) as explained by D'Amico et al. (2018). Consequently, it has been shown that higher damage states could be observed before than others.

In particular, compared to previous research, this study generated fragility curves taking into account damage to the tank wall lower course and the tank base plate with finite element analysis. For this purpose, the regression analysis made with respect to Eq. (6-1) for both EFB at the tank wall lower course and the plastic rotation at the base plate of the tank, as shown in Figure 6.4 and Figure 6.5, respectively. The Figure 6.4 shows the PGA(g) as an IM versus compressive meridional stress at the lower course of the tank wall. Besides, Figure 6.5 shows the PGA(g) as an IM versus plastic rotation for the base plate and wall-to-base connection rupture at the storage tank.

The dispersion of the demand evaluated as formulated by Eq. (6-2) using the structural response shown in Figure 6.4 and Figure 6.5. Moreover, if the material properties of the tank are calculated from the experimental tests, β_{LS} is considered 0. However, if an experiment has not been performed to determine the material properties of the tank, the capacity dispersion value of 0.5, recommendation made in FEMA (2018), is taken into account for selected failure criteria. To demonstrate the effect of β_{LS} on fragility curve both $\beta_{LS} = 0$ and $\beta_{LS} = 0.5$ is considered as shown in Figure 6.6 and Figure 6.7, respectively. Therefore, as can be understood from Figure 6.6 and Figure 6.7 below, EFB occurred early before the plastic rotation, which again proves that the damage states specified in the liquid storage tanks are not in sequence. Also, Bakalis et al. (2017), Bakalis et al. (2019) and Razzaghi & Eshghi (2008) shows that the EFB occurs before plastic rotation for broad tanks $\left(\frac{H_L}{R} > 1\right)$.

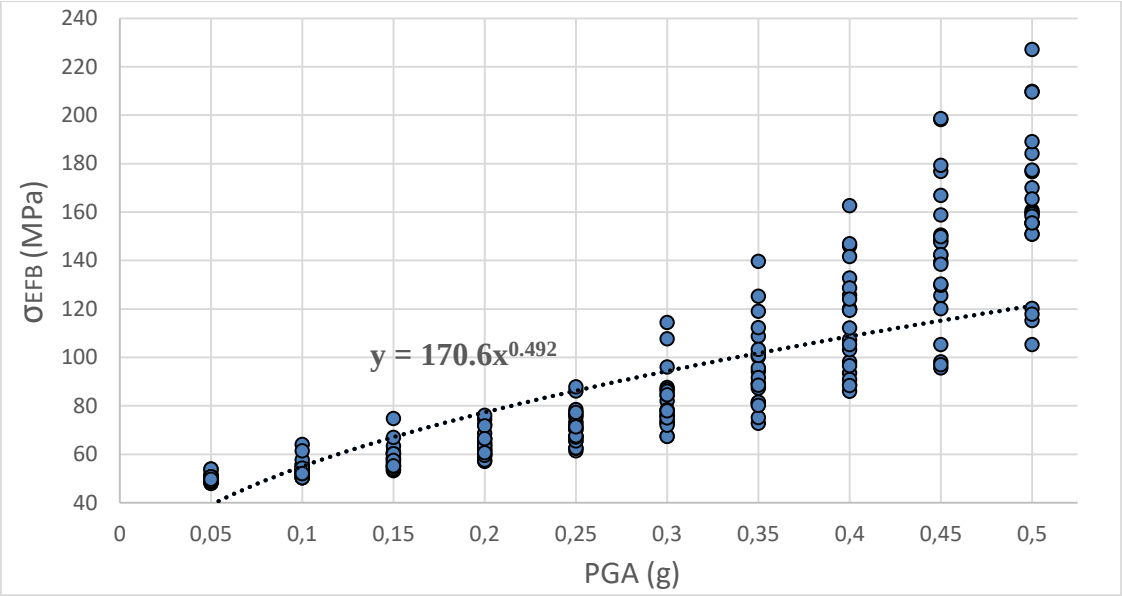

Figure 6.4 Regression analyses result for EFB at the lower course of the tank

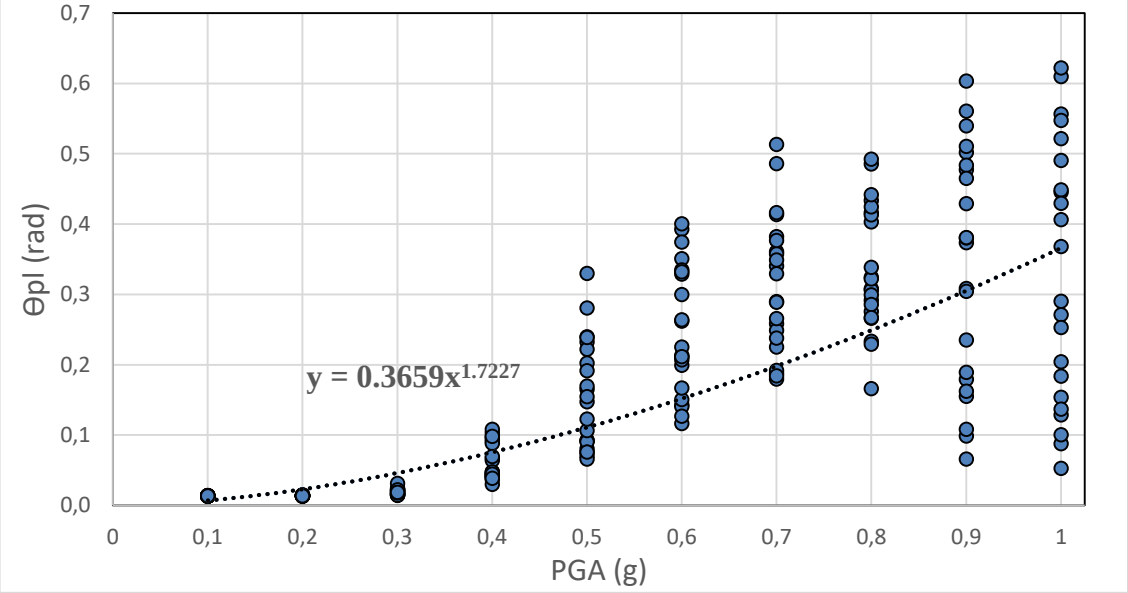

Figure 6.5 Regression analyses result for plastic rotation at the base plate of the tank

Fragility curves based on the various IMs shown in Table 5.2 are built to identify damage states and to calculate the corresponding probability of occurrence. Among magnitude-dependent IMs, PGA shows the best performance with respect to the maximum meridional stress as stated by Phan & Paolacci (2016). Another dedicated statement to demonstrate the comparison of fragility curves made by Cortes & Prinz (2016), which shows local buckling of the tank shell is more likely than ultra-low-cycle fatigue fracture of the shell-to-base connection for all geometries (both slender and broad)

and earthquake intensities considered. Consequently, as explained previous studies, the EFB probability of failure is higher than the plastic rotation probability of failure as shown in Figure 6.6 and Figure 6.7.

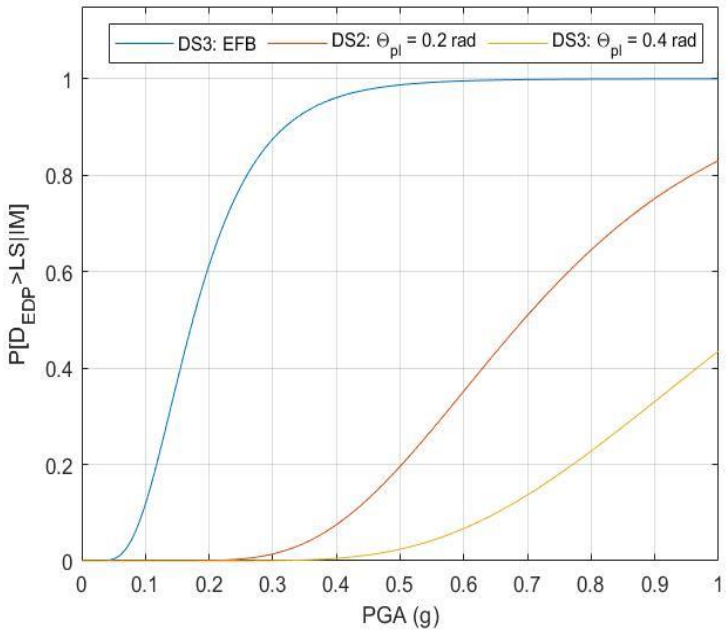

Figure 6.6 Fragility curves ($\beta_{LS} = 0$) based on EFB at the lower course of the tank wall and plastic rotation at the base of the tank

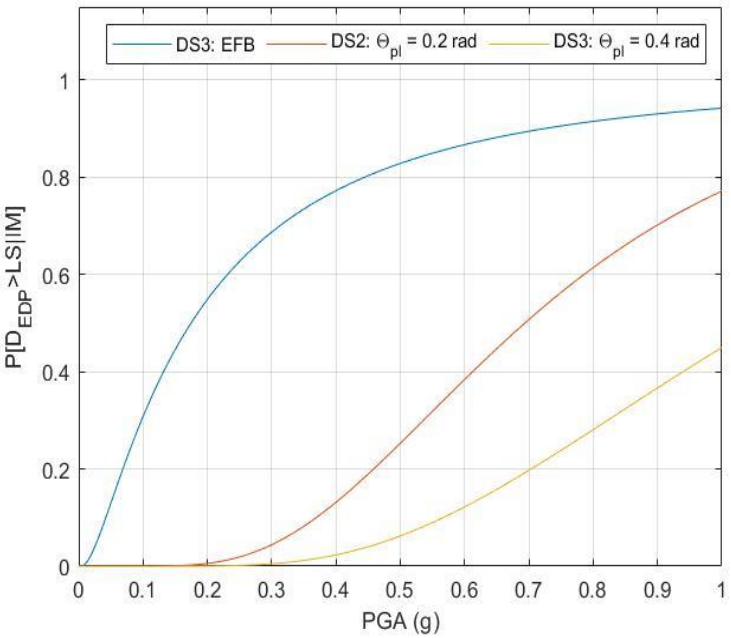

Figure 6.7 Fragility curves ($\beta_{LS} = 0.5$) based on EFB at the lower course of the tank wall and plastic rotation at the base of the tank

Moreover, the choice of this model and the corresponding variables is presented theoretically for the selected failure criteria. For EFB, as shown in Figure 6.6 and Figure 6.7, the 50% failure probability occurs when the IM is less than 0.2g. Also, the influence of the uncertainty on fragility curve of the selected failure criteria could comparable. When the uncertainty on capacity is considered, the probability of failure decrease and IM of %100 failure is increase. The fragility curves in Figure 6.6 and Figure 6.7 are evaluated with considering the ground motion uncertainty. Besides, the fragility curves in Figure 6.7 are evaluated with considering the uncertainty in material properties, and ground motion.

In this study, for the fragility curve evaluation of the selected storage tank model, the dispersion of capacity and demand considered to demonstrate the structural performance. The model's fragility curve is shown in Figure 6.7 and Figure 6.6 with respect to considered and ignored the dispersion of the structural capacity limit state, respectively. As a result, the considering uncertainties effect the fragility curves' probability of failure for selected failure criteria. Also, this demonstrates that the occurrence probability of the EFB failure mode is more than the base plate and wall-to-base connection rupture. Therefore, from the selected failure modes, the prominent failure mode is the EFB for this liquid storage tank.

CHAPTER 7

SUMMARY, CONCLUSIONS AND RECOMMENDATIONS

7.1 Summary

In the previous sections, technical information is provided to apply a PBEE driven approach for seismic performance evaluation of liquid storage tanks and to create the necessary structural components to identify potential errors explained as follows. In light of this information, a brief introduction summarizing the seismic responses as well as the design and construction applications of liquid storage tanks is made in Chapter 2. At this stage, besides the types of liquid storage tanks, the types of damage that occurred during historical earthquakes are also explained. The lessons learned from these earthquakes had a significant impact on the development of liquid storage tank design codes. Nevertheless, extensive literature studies on the dynamic analysis of liquid storage tanks have been continued, and current usage standards have been reviewed, and the literature research section has been completed. Chapter 3 covers the examination of failure modes that have been occurred in the past major earthquakes. Also, the formulations frequently used in the literature to determine these failure modes and recommended for calculating the limit state specified in the standards are presented in this section. In Chapter 4, the three-dimensional modelling technique used with detailed FEA to calculate the response of the unanchored circular liquid storage tank. Also, the main subject of this study is the assignment of both liquid and soil-structure interactions to the model. The fluid-structure interaction of the model is considered as impulsive hydrodynamic pressure, which is applied to the wall surface and the base plate of the storage tank in the reverse direction of the earthquake in the time-history analysis. Besides, the soil-structure interaction between the tank and the rigid foundation has considered during analysis with respect to the methodology defined by API 650. Consequently, detailed modelling with the use of finite element software ABAQUS is explained, as the calculation of the seismic behaviour of the tanks is complex. In order to apply the modelling technique described in Chapter 4 to the IDA calculations of nonlinear analysis, a detailed description has been made in Chapter 5. To fully understand the response of this type of model, the PBEE and FEMA P695 principles applied in this study. The main subject of this section is the scaling and

normalization of the selected earthquake data. Necessary steps have been considered for nonlinear analysis, and the results are presented in the graph. A more detailed representation of earthquake damage in liquid storage tanks was determined using the fragility curves and system performance levels presented in Chapter 6 using the PBEE methodology. Damage levels and formation mechanisms are explained respectively. The performance of the model has examined by creating fragility curves.

7.2 Conclusions

A highly complex model needs to be analyzed in the seismic analysis of unanchored liquid storage tanks, taking into account the interaction of soil structure and fluid-structure. It is therefore inevitable that the specified interactions will be used in the calculations for the seismic response assessment in order to produce a resilient structural model. With these in mind, it is understood that a different modelling approach is inevitable for the seismic response evaluation of liquid-containing structures.

Moreover, for structural response calculations, a detailed analysis of liquid storage tanks should be conducted. Therefore, the study of a combined multi-physical system is often needed to understand such a liquid storage tank system's behavior. Also, the forces on the containers during an earthquake, which are hydrodynamic and hydrostatic liquid pressure, has taken into account in the calculations as they play a key role in the safe and robust analysis of the tanks. This hydrodynamic pressure is a combination of impulsive and convective pressure. Also, in order to evaluate structural response of liquid storage tank according to the selected failure criteria, the relevant component of the hydrodynamic pressure must be considered in the calculations. Therefore, for this study with respect to selected failure criteria, the impulsive pressure distribution for liquid storage tank has considered in time history analysis to simulate the interaction of liquid-structure, and also, the impulsive pressure variation has considered during the simulation. Moreover, during the analysis of the model in a time domain, the hydrodynamic fluid pressure changes over time with respect to the acceleration of the earthquake as shown in Eq. (4-2).

In this study, the analysis of the model has been made by taking into account the effect of the crude oil inside the unanchored cylindrical liquid storage tank. Also, this section summarizes the results of the performance-based evaluation of seismic analysis

by applying the horizontal component of ground motion to unanchored cylindrical liquid storage tanks. Therefore, the methodology applied in this research has based on the principles of PBEE, and the FEMA (2009). The tanks were excited by the acceleration of scaled ground motion data of selected set with respect to FEMA (2009) to apply IDA methodology. The selected structural response for IDA is the lower course compressive meridional stress and the plastic rotation at the base plate of the liquid storage tank. Also, the variability in multi-record IDA response leads to the need for statistical treatment to demonstrate effectively in a predictive PBEE context. In addition, the IDA approach also corresponds to both demand and capacity. Finally, based on the findings of the investigation, the following results could be made:

1. This thesis introduces the impulsive hydrodynamic pressure approach to address the dynamics of a seismically excited tank-liquid system. On deriving the impulsive hydrodynamic liquid pressure shape function, the variation of the hydrodynamic pressure must be considered in the three-dimensional model. Also, the impulsive hydrodynamic pressure has been observed to exhibit a three-dimensional change in horizontal and vertical directions.
2. The structural model is divided into three subsystems in the adopted solution approach, which are the storage tank, foundation, and the contained liquid (as an impulsive pressure). Therefore, the impulsive component of liquid pressure had taken into account for the analysis used in this study. When the tank is induced to earthquake ground motion in the horizontal direction, the pressure at junction of the base plate and wall gives the highest pressure at the wall.
3. The dynamic behaviour, as well as fluid-structure interaction, depends on the model geometry and the volume of the liquid in the storage tank. Consequently, the shell thickness and the bottom plate, as well as the liquid level, had the most critical impact on the structural dynamic response.
4. The finite element analysis model proposed in this study considers the effect of tank flexibility in each time-history analysis. Also, the developed FEM has been used to analyze the influence of PGA on the structural behaviour as an IM of earthquake ground motion data. In this way, the effect of different modes that may occur has been taken into account in the calculations.
5. Fragility curves have been obtained for two selected failure modes, the EFB and the plastic rotation of the shell-to-bottom plate joint. Also, DS2 and DS3 considered for the plastic rotation of the shell-to-bottom plate. Finally, EFB

has shown a higher occurrence probability compared with those caused by the plastic rotation of the shell-to-bottom plate. Therefore, EFB is the prominent failure mode within selected failure criteria for this model.

6. The results of analyses obtained using the analytical – finite element models, full FEM based on the ABAQUS system is consistent. In general, from the results of the study of the tank seismic response, with the help of the finite element software ABAQUS, we were able to understand the different responses of the unanchored liquid storage tank.

In conclusion, the application of the PBEE framework for liquid storage tanks has extensively been discussed. Using the appropriate component and system-level damage state classifications for individual tanks, the vulnerability of liquid storage tanks against earthquakes is revealed, as even ground motions with 0.30g PGA may result in significant damage. Adopting state-of-the-art, intensity measures do not alter the conclusions as mentioned above, yet it provides a more robust tool to assess seismic performance.

7.3 Recommendations

In this study, a limited number of failure criteria of unanchored liquid storage tank are taken into consideration. Therefore, detailed analysis considering all failure criteria would allow the tank to evaluate a more reliable structural performance class for the overall performance evaluation of the liquid storage tank.

For a detailed explanation of EFB, it is conceivable for different dimensions of circular fluid storage tanks with variable fluid height to show this failure criterion in more detail.

To understand the criteria for failure of foundation and soil properties under seismic simulation, the presumed type of foundation can be considered included along with selected site soil conditions and basic material properties. Modeling of the soil and the foundation with their real characteristics will provide an accurate calculation of the structural response. Therefore, researchers can work on soil-supported storage tanks and compare detailed models with simple models proposed in the literature.

To consider sloshing phenomena in the liquid storage tanks different modelling techniques could be used to get structural response. The behaviour of a model at the upper

part could be evaluated to check the sloshing phenomena impact on the given failure criteria related to the sloshing.

The effect of the aspect ratio on the seismic response of liquid storage tanks could be explained by considering various aspect ratios.

REFERENCES

ABAQUS. Version 2019. Dassault Systèmes

Ahari, Masoud Nourali, Sassan Eshghi, and Mohsen Ghafory Ashtiany. "The Tapered Beam Model for Bottom Plate Uplift Analysis of Unanchored Cylindrical Steel Storage Tanks." *Engineering Structures* 31, no. 3 (2009): 623-32. https://doi.org/10.1016/j.engstruct.2008.10.011.

AIJ. *Design Recommendation for Storage Tanks and Their Supports with Emphasis on Seismic Design.* 2010.

ALA. *Seismic Fragility Formulations for Water Systems.* ASCE, 2001.

Alembagheri, M., and H.E. Estekanchi. "Nonlinear Analysis of Aboveground Anchored Steel Tanks Using Endurance Time Method." (2011).

Altun, Haluk Alper. "Seismic Analysis of Steel Liquid Storage Tanks by Api-650." Master of Science, Istanbul Technical University, 2013.

API. *Welded Steel Tanks for Oil Storage.* 2007.

API. *Welded Steel Tanks for Oil Storage.* 1998.

ASCE. *Guidelines for Seismic Evaluation and Design of Petrochemical Facilities.* 2010.

Avval, Ima T. "Dynamic Response of Concrete Rectangular Liquid Tanks in Three-Dimensional Space." Master of Applied Science, Tabriz University, 2012.

Bakalis, Konstantinos. "Seismic Performance Assessment of Industrial Facility Atmospheric Liquid Storage Tanks." Doctoral Thesis, National Technical University of Athens, 2018.

Bakalis, Konstantinos, Michalis Fragiadakis, and Dimitrios Vamvatsikos. "Surrogate Modeling of Liquid Storage Tanks for Seismic Performance Design and Assessment." (2015). https://doi.org/10.7712/120115.3523.1375.

Bakalis, Konstantinos, Athanasia K. Kazantzi, Dimitrios Vamvatsikos, and Michalis Fragiadakis. "Seismic Performance Evaluation of Liquid Storage Tanks Using Nonlinear Static Procedures." *Journal of Pressure Vessel Technology* 141, no. 1 (2019). https://doi.org/10.1115/1.4039634.

Bakalis, Konstantinos, Dimitrios Vamvatsikos, and Michalis Fragiadakis. "Seismic Fragility Assessment of Steel Liquid Storage Tanks." (2015).

Bakalis, Konstantinos, Dimitrios Vamvatsikos, and Michalis Fragiadakis. "Seismic Risk Assessment of Liquid Storage Tanks Via a Nonlinear Surrogate Model." *Earthquake Engineering & Structural Dynamics* 46, no. 15 (2017): 2851-68. https://doi.org/10.1002/eqe.2939.

Barros, R. C. "Preliminary Seismic Analysis and Design of Liquid Storage Tanks." (1987).

Buratti, N., and Matteo Tavano. "Dynamic Buckling and Seismic Fragility of Anchored Steel Tanks by the Added Mass Method." (2014). https://doi.org/10.1002/eqe.2326

CEN. *Eurocode 8: Design of Structure for Earthquake Resistance ─ Part 4: Silos, Tanks and Pipelines.* Brussels, Belgium: European Committee for Standardization, 2006.

Chen, Jun Zheng. "Generalized Sdof System for Dynamic Analysis of Concrete Rectangular Liquid Storage Tanks." Doctor of Philosophy, Ryerson University, 2010.

Christovasilis, Ioannis P. "Seismic Analysis of Liquefied Natural Gas Tanks." Master of Science, State University of New York, 2006.

Cimellaro, Gian Paolo, Andrei M. Reinhorn, Michel Bruneau, and Avigdor Rutenberg. *Multi Dimentional Fragility of Structures Formulation and Evaluation.* (2006).

Colombo, J. I., and J. L. Almazán. "Simplified 3d Model for the Uplift Analysis of Liquid Storage Tanks." *Engineering Structures* 196 (2019). https://doi.org/10.1016/j.engstruct.2019.109278.

Cortes, Gustavo, and Gary S. Prinz. "Seismic Fragility Analysis of Large Unanchored Steel Tanks Considering Local Instability and Fatigue Damage." *Bulletin of Earthquake Engineering* 15, no. 3 (2016): 1279-95. https://doi.org/10.1007/s10518-016-9984-6.

Cortes, Gustavo, Gary S. Prinz, Alain Nussbaumer, and Martin G. Koller. "Cyclic Demand at the Shell-Bottom Connection of Unanchored Steel Tanks." (2012).

Cortes, Gustavo, Alain Nussbaumer, and Martin Coller. "Seismic Behavior of Shell-Base Connections in Large Storage Tanks." (2011).

Çelik, Ali İhsan, Mehmet Metin Köse, Tahir Akgül, and Ahmet Celal Apay. "Effects of the Shell Thickness on the Directional Deformation and Buckling on the Cylindrical Steel Water Tanks under the Kobe Earthquake Loading." *Sakarya University Journal of Science* (2019): 1-1. https://doi.org/10.16984/saufenbilder.423872.

D'Amico, Marta, Luca Vittuari, Claudio Mazzotti, and Nicola Buratti. "Seismic Fragility and Dynamic Behavior of Atmospheric Cylindrical Steel Tanks." Doctor of Philosophy, University of Bologna, 2018.

Dogangun, Adem, Zeki Karaca, Ahmet Durmus, and Halil Sezen. "Cause of Damage and Failures in Silo Structures." (2009). https://doi.org/10.1061/(ASCE)0887-3828(2009)23:2(65).

Erkmen, Bulent. "Evaluation of Code Provisions for Seismic Performance of Unachored Liquid Storage Tanks." Proceedings of the 6th International Conference on Computational Methods in Structural Dynamics and Earthquake Engineering (COMPDYN 2015), 2017.

Estekanchi, Homayoon Estekanchi, Abbas Ali Vafaei, and M. Sadeghazar. "Endurance Time Method for Seismic Analysis and Design of Structures." (2004).

FEMA. *Nehrp Guidelines for the Seismic Rehabilitation of Buildings.* 1997.

FEMA. *Qualification of Building Seismic Performance Factor.* Washington, D.C.: Federal Emergency Management Agency, 2009.

FEMA. *Seismic Performance Assessment of Buildings: Volume 1—Methodology.* Redwood City, CA: APPLIED TECHNOLOGY COUNCIL, 2018.

Ghaemmaghami, Amirreza. "Dynamic Time-History Response of Concrete Rectangular Liquid Storage Tanks." Doctor of Philosophy, Sharif University, 2002.

Habenberger, Joerg "Fluid Damping of Cylindrical Liquid Storage Tanks." *Springerplus* 4 (2015): 515. https://doi.org/10.1186/s40064-015-1302-2. https://www.ncbi.nlm.nih.gov/pubmed/26405635.

Hafez, Ahmet. "Seismic Response of Ground Supported Circular Concrete Tanks." Doctor of Philosophy, Ryerson University, 2012.

Haroun, Medhat A., and M. A. Al-Kashif. "Merhodology for Design of Earthquake Resistant Steel Liquid Storage Tanks." (2005). https://doi.org/10.2495/ERES050641.

Haroun, Medhat A., and G. W. Housner. "Earthquake Response of Deformable Liquid Storage Tanks." (1981). https://doi.org/https://doi.org/10.1115/1.3157631.

Haroun, Medhat A. "Mitigation of Elephants Foot Bulge Formation in Seismically-Excited Steel Storage Tanks." (2005).

Haroun, Medhat A. "Vibration Studies and Tests of Liquid Storage Tanks." (1983).

HAZUS. *Fema-Nibs Multi-Hazard Loss Estimation Methodology - Hazus-Mh Mr5 Earthquake Model Technical Manual.* Washington, D.C.: Federal Emergency Management Agency, 2010.

HAZUS. *Hazus-Mh 2.1 Technical Manual: Earthquake Model.* Washington, D.C.: Department of Homeland Security, Federal Emergency Management Agency, 2014.

Housner, G. W. "The Dynamic Behavior of Water Tanks." (1963).

Housner, G. W. "Dynamic Pressures on Accelerated Fluid Containers." (1954).

Jaiswal, O. R, and Sudhir K Jain. "Modified Proposed Provisions for Aseismic Design of Liquid Storage Tanks." (2005).

Jing, Wei, Huan Feng, and Xuansheng Cheng. "Dynamic Responses of Liquid Storage Tanks Caused by Wind and Earthquake in Special Environment." *Applied Sciences* 9, no. 11 (2019). https://doi.org/10.3390/app9112376.

Karim, Abdulamir Atalla. "Vibration Analysis of Circular Cylindrical Liquid Storage Tanks Using Finite Element Technique." Doctor of Philosophy, University of Basrah, 2008.

Koller, Martin G., and Praveen K. Malhotra. "Seismic Evaluation of Unanchored Cylindrical Tanks." (2004).

Kwon, Young W. *Multiphysics and Multiscale Modeling: Techniques and Applications.* 2015.

Lee, Sangmok, Byungmin Kim, and Young-Joo Lee. "Seismic Fragility Analysis of Steel Liquid Storage Tanks Using Earthquake Ground Motions Recorded in Korea." *Mathematical Problems in Engineering* 2019 (2019): 1-15. https://doi.org/10.1155/2019/6190159.

Malhotra, Praveen K. "Base Uplifting Analysis of Flexibly Supported Liquid Storage Tanks." (1995). https://doi.org/10.1002/eqe.4290241204.

Malhotra, Praveen K. "Seismic Response of Soil-Supported Unanchored Liquid-Storage Tanks." (1997). https://doi.org/10.1061/(ASCE)0733-9445(1997)123:4(440).

Malhotra, Praveen K. "Seismic Response of Uplifting Liquid Storage Tanks." Doctor of Philosophy, Rice University, 1992.

Malhotra, Praveen K., and Anestis S. Veletsos. "Beam Model for Base-Uplifting Analysis of Cylindrical Tanks." (1994). https://doi.org/10.1061/(ASCE)0733-9445(1994)120:12(3471).

Malhotra, Praveen K., and Anestis S. Veletsos. "Uplifting Analysis of Base Plates in Cylindrical Tanks." *Journal of Structural Engineering* 120, no. 12 (1994): 3489-505. https://doi.org/10.1061/(asce)0733-9445(1994)120:12(3489).

Malhotra, Praveen K., and Anestis S. Veletsos. "Uplifting Response of Unanchored Liquid-Storage Tanks." (1994). https://doi.org/10.1061/(ASCE)0733-9445(1994)120:12(3525).

Malhotra, Praveen K. "Practical Nonlinear Seismic Analysis of Tanks." *Earthquake Spectra* 16, no. 2 (2000): 473-92. https://doi.org/10.1193/1.1586122.

Malhotra, Praveen K., Thomas Wenk, and Martin Wieland. "Simple Procedure for Seismic Analysis of Liquid Storage Tanks." (2000). https://doi.org/10.3929/ethz-a-006032188

Mangalathu, Sujith, Eunsoo Choi, Han Cheol Park, and Jong-Su Jeon. "Probabilistic Seismic Vulnerability Assessment of Tall Horizontally Curved Concrete Bridges in California." *Journal of Performance of Constructed Facilities* 32, no. 6 (2018). https://doi.org/10.1061/(asce)cf.1943-5509.0001231.

Manos, Cloud. *Further Study of the Earthquake Response of a Broad Cylindrical Liquid-Storage Tank Model.* 1982.

Meskouris, Konstantin, Christoph Butenweg, Klaus-G. Hinzen, and Rüdiger Höffer. *Structural Dynamics with Applications in Earthquake and Wind Engineering.* 2019. doi:10.1007/978-3-662-57550-5.

Moslemi, Mehdi. "Seismic Response of Ground Cylindrical and Elevated Conical Concrete Tanks." Doctor of Philosophy, Ryerson University, 2011.

Nielson, Bryant G., and Reginald DesRoches. "Analytical Seismic Fragility Curves for Typical Bridges in the Central and Southeastern United States." *Earthquake Spectra* 23, no. 3 (2019): 615-33. https://doi.org/10.1193/1.2756815.

NZSEE. *Seismic Design of Storage Tanks.* New Zealand Society for Earthquake Engineering, 2009.

Ormeno, Miguel, Tam Larkin, and Nawawi Chouw. "Influence of Uplift on Liquid Storage Tanks During Earthquakes." (2012).

Ozdemir, Z., M. Souli, and Y. M. Fahjan. "Application of Nonlinear Fluid–Structure Interaction Methods to Seismic Analysis of Anchored and Unanchored Tanks." *Engineering Structures* 32, no. 2 (2010): 409-23. https://doi.org/10.1016/j.engstruct.2009.10.004.

Ozdemir, Zuhal, Mhamed Souli, and M. Fahjan Yasin. "Numerical Evaluation of Nonlinear Response of Broad Cylindrical Steel Tanks under Multidimensional Earthquake Motion." *Earthquake Spectra* 28, no. 1 (2020): 217-38. https://doi.org/10.1193/1.3672996.

Pantusheva, Maria "Seismic Analysis of Steel Storage Tanks Overview of Design Codes Used in Practice." (2017).

Phan, Hoang Nam, and Fabrizio Paolacci. "Efficient Intensity Measures for Probabilistic Seismic Response Analysis of Anchored above-Ground Liquid Steel Storage Tanks." Volume 5: High-Pressure Technology; Rudy Scavuzzo Student Paper Symposium and 24th Annual Student Paper Competition; ASME Nondestructive Evaluation, Diagnosis and Prognosis Division (NDPD); Electric Power Research Institute (EPRI) Creep Fatigue Workshop, 2016.

Phan, Hoang Nam, and Fabrizio Paolacci. "Fluid-Structure Interaction Problems: An Application to Anchored and Unanchored Steel Storage Tanks." (2018).

Phan, Hoang Nam, Fabrizio Paolacci, and Silvia Alessandri. "Enhanced Seismic Fragility Analysis of Unanchored Steel Storage Tanks Accounting for Uncertain Modeling Parameters." *Journal of Pressure Vessel Technology* 141, no. 1 (2019). https://doi.org/10.1115/1.4039635.

Phan, Hoang Nam, Fabrizio Paolacci, Daniele Corritore, and Silvia Alessandri. "Seismic Vulnerability Analysis of Storage Tanks for Oil and Gas Industry." (2018). https://doi.org/10.28999/2514-541X-2018-2-1-55-65.

Phan, Hoang Nam, Fabrizio Paolacci, Daniele Corritore, Nicola Tondini, and Oreste S. Bursi. "A Kriging-Based Surrogate Model for Seismic Fragility Analaysis of

Unanchored Storage Tanks." (2019). https://doi.org/https://doi.org/10.1115/PVP2019-93259.

Porter, Keith. *A Beginner's Guide to Fragility, Vulnerability, and Risk.* 2020. doi:10.1007/978-3-642-36197-5_256-1.

Prasad, Anumolu Meher, Veletsos. "Studies of Soil-Structure and Fluid-Structure Interaction." Doctor of Philosophy, Rice University, 1989.

Priestley, M. J. N. "Analysis and Design of Circular Prestressed Concrete Storage Tanks." (1985).

Rammerstorfer, Franz G., Knut Scharf, and Franz D. Fisher. "Storage Tanks under Earthquake Loading." (1990). https://doi.org/https://doi.org/10.1115/1.3119154.

Rashed, Ahmed A., Gamal H. Mahmoud, Nasr E. Nasr, and Amgad A. Talaat. "3d Analysis for Conical Tanks under Seismic Loads." (2019). https://doi.org/10.9790/1684-1601012944.

Rawat, Aruna, Vasant A. Matsagar, and A. K. Nagpal. "Numerical Study of Base-Isolated Cylindrical Liquid Storage Tanks Using Coupled Acoustic-Structural Approach." *Soil Dynamics and Earthquake Engineering* 119 (2019): 196-219. https://doi.org/10.1016/j.soildyn.2019.01.005.

Rawat, Aruna, Vasant Matsagar, and A.K. Nagpal. "Coupled Acoustic-Structure Interaction in Cylindrical Liquid Storage Tank Subjected to Bi-Directional Excitation." Chap. Chapter 90 In *Advances in Structural Engineering*, 1155-66, 2015.

Rawat, Aruna, Vasant Matsagar, and A.K. Nagpal. "Finite Element Simulation of Cylindrical Liquid Storage Tank under Tri-Directional Components of Earthquake." (2015). https://doi.org/10.3850/978-981-09-1139-3_089.

Rawat, Aruna, Vaibhav Mittal, Tanusree Chakraborty, and Vasant Matsagar. "Earthquake Induced Sloshing and Hydrodynamic Pressures in Rigid Liquid Storage Tanks Analyzed by Coupled Acoustic-Structural and Euler-Lagrange Methods." *Thin-Walled Structures* 134 (2019): 333-46. https://doi.org/10.1016/j.tws.2018.10.016.

Razzaghi, Mehran Seyed, and Sassan Eshghi. "Development of Analytical Fragility Curves for Cylindrical Steel Oil Tanks." (2008).

Rostami, N. Khakzad, and P. H. A. J. M van Gelder. *Post-Emergency, Multi-Hazard Health Risk Assessment in Chemical Disasters (Pec): Report on the Evaluation of Possible Damages Suffered by Chemical and Process Vessels Due to Floods.* (2017).

Sezen, Halil, and Andrew S. Whittaker. "Performance of Industrial Facilities During the 1999, Kocaeli, Turkey Earthquake." (2004).

Sobhan, M. S., Fayaz R. Rofooei, and Nader K. A. Attari. "Buckling Behavior of the Anchored Steel Tanks under Horizontal and Vertical Ground Motions Using

Static Pushover and Incremental Dynamic Analyses." *Thin-Walled Structures* 112 (2017): 173-83. https://doi.org/10.1016/j.tws.2016.12.022.

Soules, J. Greg. *Guidelines for Seismic Evaluation and Design of Petrochemical Facilities.* 2011.

Tavano, Matteo. "Seismic Response of Tank-Fluid Systems Dynamic Buckling Analysis of a Steel Tank with the Added Mass Method." Università degli Studi di Bologna, 2011.

Teng, Jin-Guang, and J. M. Rotter. *Buckling of Thin Metal Shells.* 2004.

Vakilazadsarabi, Ali. "Sloshing Fenomena in Water Reservoir Tanks Due to Long Period-Long Duration Earthquake Ground Motions." 2014.

Vamvatsikos, Dimitrios. "Seismic Performance, Capacity and Reliability of Structures as Seen through Incremental Dynamic Analysis." 2002.

Vathi, Karamanos. "Modeling of Uplifting Mechanism in Unanchored Liquid Storage Tanks Subjected to Seismic Loading." (2014).

Vathi, Karamanos. "A Simple and Efficient Model for Seismic Response and Low-Cycle Fatique Assesment of Uplifting Liquid Storage Tanks." (2017). https://doi.org/10.1016/j.jlp.2017.08.003.

Vathi, Maria, and Spyros A. Karamanos. "Simplified Model for the Seismic Performance of Unanchored Liquid Storage Tanks." (2015). https://doi.org/10.1115/PVP2015-45695.

Veletsos, Anestis S. *Seismic Response and Design of Liquid Storage Tanks.* 1984.

Veletsos, Anestis S., and Carlos E. Ventura. "Efficient Analysis of Dynamic Response of Linear Systems." (1984). https://doi.org/10.1002/eqe.4290120408.

Virella, Juan C., Luis A. Godoy, and Luis E. Suarez. "Effect of Pre-Stress States on the Impulsive Modes of Vibration of Cylindrical Tank-Liquid Systems under Horizontal Motions." *Journal of Vibration and Control* 11, no. 9 (2005): 1195-220. https://doi.org/10.1177/1077546305057221.

Virella, Juan C., Luis A. Godoy, and Luis E. Suarez. "Fundamental Modes of Tank-Liquid Systems under Horizontal Motions." *Engineering Structures* 28, no. 10 (2006): 1450-61. https://doi.org/10.1016/j.engstruct.2005.12.016.

Yazdanian, M., and Sadegh Ghasemi. "Study on Fundamental Frequencies of Cylindrical Storage Tanks Obtained from Codes and Finite Element Method." (2017). https://doi.org/10.7508/ceij.2017.01.008.

Yazıcı, Gökhan. "Sismik Yalıtımlı Düşey Silindirik Sıvı Depolarının Deprem Yükleri Altındaki Davranışının İncelenmesi." Doctor of Philosophy, Istanbul Technical University, 2008.

Zareian, Farzin, Carlos Sampere, Victor Sandoval, David L. McCormick, Jack Moehle, and Roberto Leon. "Reconnaissance of the Chilean Wine Industry Affected by

the 2010 Chile Offshore Maule Earthquake." *Earthquake Spectra* 28, no. 1_suppl1 (2020): 503-12. https://doi.org/10.1193/1.4000048.